Spin-Lattice Relaxation in Some Rare-Earth Salts at Helium Temperatures; Observation of the Phonon Bottleneck*†

P. L. Scott‡ AND C. D. Jeffries§

Department of Physics, University of California, Berkeley, California

(Received February 19, 1962)

By observing the transient recovery of microwave paramagnetic resonance signals at $\nu \approx 9.3$ kMc/sec and $\nu \approx 34$ kMc/sec, we measure the spin-lattice relaxation rate T_1^{-1} for the rare earth ions Nd, Pr, and Sm in the double nitrate [$La_2Mg_3(NO_3)_{12} \cdot 24H_2O$] and for Ce and Nd in the ethyl sulfate [$La(C_2H_5SO_4)_3 \cdot 9H_2O$] in the temperature range $1.4° < T < 5°K$. We observe the direct process, $T_1^{-1} \propto T$; the Orbach process, $T_1^{-1} \propto \exp(-\Delta/kT)$; and the Raman process, $T_1^{-1} \propto T^7$ and T^9. The measured relaxation rates are in good agreement with simple theoretical estimates based on Orbach's phenomenological approach. For example, for 1% Nd in the ethyl sulfate with $z \perp H$ at $\nu = 9.3$ kMc/sec we measure $T_1^{-1} = 1.7T + 3.6 \times 10^{-4}T^9$ sec^{-1}, as compared to the theoretical estimate, $T_1^{-1} = 1.4T + 1.3 \times 10^{-4}T^9$ sec^{-1}. The data, together with similar measurements by others, lead to the over-all conclusion that spin-lattice relaxation at low temperatures in rare earth salts is reasonably well understood.

At the lowest temperatures, where the direct process dominates, we observe in the double nitrate several instances of a spin-bath relaxation rate T_b^{-1} which is not the direct spin-lattice (i.e., spin-phonon) process, but rather a slower phonon-limited "bottle-neck" process, with a temperature dependence $T_b^{-1} \propto T^2$. This dependence along with that on crystal size and paramagnetic ion concentration is in good agreement with simple theoretical expectations. The data indicate that the hot phonon-bath relaxation time is the time taken by sound waves to traverse the crystal half-thickness. For 1% Pr in the double nitrate at 1.4°K the bottleneck is severe, the observed rate T_b^{-1} being $\sim 10^3$ times smaller than the true direct rate T_1^{-1}.

I. INTRODUCTION

THE classic papers of Waller,[1] Heitler and Teller,[2] Van Vleck,[3] Kronig,[4] and others have shown that the dominant spin-lattice interaction of paramagnetic ions in crystals is through the thermal modulation of the crystalline electric field. The theory generally predicts that at very low temperatures, T, the spin-lattice relaxation time T_1 will be determined by the direct process, where $T_1^{-1} \propto T$; and at the upper helium temperatures by the Raman process, where $T_1^{-1} \propto T^7$ or $T_1^{-1} \propto T^9$. The agreement between predicted and measured relaxation times for iron group ions has not been very satisfactory in the past, probably because of complicating factors such as spin-spin interactions in magnetically concentrated crystals, cross relaxation,[5] and phonon heating effects.[6-8]

Because of the close relation to masers, microwave phonon experiments, dynamic nuclear orientation, etc., there has been renewed interest in the problem of spin-lattice relaxation in recent years. The theory has been re-examined by Mattuck and Strandberg[9] for the iron group. Relaxation in the rare earths has been considered theoretically in a detailed paper by Orbach,[10] who uses a simple phenomenological approach to estimate relaxation times. He also finds a process to explain the rapid exponential temperature dependence, $T_1^{-1} \propto \exp(-\Delta/kT)$, observed in some rare earth salts.[11]

In order to further check experiment with theory, we have observed the transient response of the microwave paramagnetic resonance absorption to thus measure the relaxation time for a number of rare earth salts, and have compared the results with our theoretical estimates, based on Orbach's phenomenological treatment. In this paper we report the results on trivalent Ce, Nd, Pr, and Sm ions in the double nitrate and in the ethyl sulfate, in the temperature range 1.4 to 5.0°K. In the following paper[13] results are given for Ce and Nd in the double nitrate in the range 0.3° to 1.5°K.

Using a simple approach and emphasizing physical concepts, in Sec. II we review briefly the theory, setting down the explicit expressions we use to estimate the *spin-lattice rate* T_1^{-1} for the direct, Raman, and Orbach processes. We consistently use the word lattice to refer to the phonons in the crystal; the word bath refers to the (liquid helium) reservoir at temperature T in which the crystal is immersed. The experiments actually measure the *spin-bath relaxation rate* T_b^{-1}, which is, of course, equal to T_1^{-1} if the phonons have the bath temperature. However, for a sufficiently rapid direct process the phonons may become hot, and the observed rate is shown to become $T_b^{-1} = DT^2 \neq T_1^{-1}$; this "phonon

* Research supported in part by the U. S. Atomic Energy Commission and the Office of Naval Research.

† Based on part of the Ph.D. dissertation of P. L. Scott, University of California, Berkeley, December, 1961.

‡ Present address: Clarendon Laboratory, Oxford, England.

§ Associate Professor at Miller Institute for Basic Research.

[1] I. Waller, Z. Physik 79, 370 (1932).

[2] W. Heitler and E. Teller, Proc. Roy. Soc. (London) 155, 629 (1936).

[3] H. Van Vleck, Phys. Rev. 57, 426 (1940).

[4] R. de L. Kronig, Physics 6, 33 (1939).

[5] N. Bloembergen, S. Shapiro, P. S. Pershan, and J. O. Artman, Phys. Rev. 114, 445 (1959).

[6] J. H. Van Vleck, Phys. Rev. 59, 724 (1941).

[7] J. A. Giordmaine, L. E. Alsop, F. R. Nash, and C. H. Townes, Phys. Rev. 109, 302 (1958); P. W. Anderson, Phys. Rev. 114, 1002 (1959).

[8] B. W. Faughnan and M. W. P. Strandberg, J. Phys. Chem. Solids 19, 155 (1961).

[9] R. D. Mattuck and M. W. P. Strandberg, Phys. Rev. 119, 1204 (1960).

[10] R. Orbach, Proc. Roy. Soc. (London) A264, 456 (1961).

[11] C. B. P. Finn, R. Orbach, and W. P. Wolf, Proc. Phys. Soc. (London) 77, 261 (1961); A. H. Cooke, C. B. P. Finn, B. W. Mangum, and R. L. Orbach, "Proceedings of International Conference on Magnetism and Crystallography, Kyoto, Japan, 1961" (to be published).

[12] J. P. Lloyd and G. E. Pake, Phys. Rev. 94, 579 (1954).

[13] R. H. Ruby, H. Benoit, and C. D. Jeffries, following paper [Phys. Rev. 126, 51 (1962)].

bottleneck" process may obscure the true spin-lattice relaxation rate T_1^{-1}, but is distinguishable from it.

In Sec. III we describe the crystals, the microwave apparatus, and our general procedure for measuring T_b^{-1}. Explicit results are given in Sec. IV for several ions, along with the theoretical estimates. The agreement is generally satisfactory. A phonon bottleneck is observed in several instances and is adequately explained. Some of this work has been briefly reported earlier.[14]

II. REVIEW OF THEORY[3,4,10,15]

For rare earth ions in the electronic ground state in crystals we take a Hamiltonian $\mathcal{H} = \mathcal{H}_{so} + \mathcal{H}_c + \mathcal{H}_z$, the terms representing the spin-orbit, crystal field, and Zeeman interactions, respectively. We omit hyperfine interaction terms by virtue of choosing isotopes with nuclear spin $I = 0$. We usually use magnetically dilute crystals and so omit spin-spin interactions. The spin-orbit splitting ($\sim 10^3$ cm^{-1}) is considerably greater than the crystal field splittings Δ_1, Δ_2, $\cdots$, ($\sim 10^2$ cm^{-1}), so that the lowest J multiplet of the free ion is split by the crystal field into a manifold of states, each of which may be approximately represented by some linear combination of the basis wave functions $|J, J_z\rangle$, where J is a good quantum number. For ions with an odd number of electrons each state has at least Kramers degeneracy, which may be removed by an external magnetic field H, resulting in a series of doublets $|a\rangle$ and $|b\rangle$, $|c\rangle$ and $|d\rangle$, etc., in Fig. 1. For ions with an even number of electrons, some of the states may be singlets, but we assume, as is often the case, that a magnetic doublet lies lowest.

We consider a single crystal of volume V containing a total of N paramagnetic ions, immersed in a liquid helium bath at temperature T and in a magnetic field H. Only the lowest magnetic doublet is significantly populated and one usually observes microwave paramagnetic resonance only between states $|a\rangle$ and $|b\rangle$, which we take to have the populations N_a and $N_b = N - N_a$, respectively. The states are separated by an energy $\delta = h\nu$, of order 1 cm^{-1}. We review below the contributions of various processes to the spin-lattice relaxation rate T_1^{-1} between these two levels, i.e., the rate at which the population difference $(N_a - N_b)$ approaches its thermal equilibrium value after a disturbance, e.g., a saturating microwave pulse.

A. The Direct Process

We imagine the *spin system* (i.e., the paramagnetic ions) to be imbedded in a crystal lattice whose thermal vibrations may be represented by the *phonon system*, i.e., a set of lattice oscillators, each with average energy $\bar{E} = (\frac{1}{2} + \bar{p})\delta$, where $\bar{p}$ is the average phonon excitation number and is used to characterize the state of the

[14] R. H. Ruby, H. Benoit, P. L. Scott, and C. D. Jeffries, Bull. Am. Phys. Soc. **6**, 512 (1961).

[15] A. Abragam, *The Principles of Nuclear Magnetism* (Oxford University Press, New York, 1961), Chap. IX, Sec. IV.
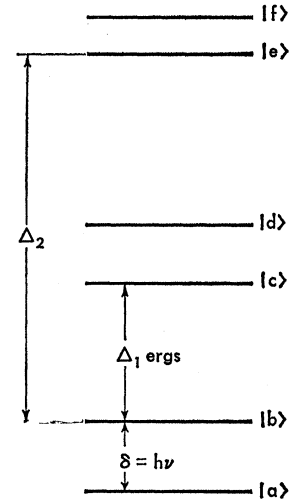
FIG. 1. Schematic energy level diagram of the lowest state of a rare earth ion in a crystalline field (splittings Δ_1, $\Delta_2 \cdots$) and in a magnetic field (splitting δ).

phonon system. We assume that the number of oscillators in the crystal with energy between δ and $\delta + d\delta$ has the classical value

$$\rho(\delta)d\delta = 3V\delta^2 d\delta / 2\pi^2 \hbar^3 v^3, \qquad (1)$$

where v is the velocity of sound. The spins are coupled to the phonons by a phenomenological Hamiltonian $\mathcal{H}_c'$ [due, e.g., to the fluctuating crystal field interaction with the orbital moment and hence to the spin by spin-orbit coupling] which acts as a time-dependent "relaxation" perturbation to produce a spin flip from state $|b\rangle$ to state $|a\rangle$, simultaneously with the creation of a phonon of energy δ, thus conserving energy. This is the direct process. We assume for the moment that the *phonon system* is very strongly coupled to the *bath* at temperature T, so that the phonon created passes on immediately to the bath; $\bar{p}$ will always have its thermal equilibrium value

$$\bar{p}_0(\delta) = [\exp(\delta/kT) - 1]^{-1}. \qquad (2)$$

In Sec. II D we consider the case $\bar{p} \neq \bar{p}_0$.

Recalling that the matrix elements for phonon creation and absorption are those of the harmonic oscillator, we write the transition probability per second for a spin flip from $|b\rangle$ to $|a\rangle$ as

$$w_{b \to a} = K[\bar{p}_0(\delta) + 1] \text{ sec}^{-1} \qquad (3a)$$

and for the reverse process

$$w_{a \to b} = K\bar{p}_0(\delta) \text{ sec}^{-1}. \qquad (3b)$$

Here, K is considered simply as a temperature-independent factor, to be evaluated later. The rate equation for the spin system can be written as

$$-\dot{N}_a = \dot{N}_b = -N_b w_{b \to a} + N_a w_{a \to b}$$
$$= K[-N_b \bar{p}_0(\delta) - N_b + N_a \bar{p}_0(\delta)]. \qquad (4)$$

The three terms on the right represent stimulated emission, spontaneous emission, and absorption of

phonons, respectively. By introducing

$$n = N_a - N_b \tag{5a}$$

and its thermal equilibrium value

$$n_0 = N \tanh(\delta/2kT), \tag{5b}$$

we obtain

$$\dot{n} = -T_{1d}^{-1}(n - n_0), \tag{5c}$$

where

$$T_{1d}^{-1} = K \coth(\delta/2kT) \tag{6}$$

is the direct spin-lattice relaxation rate. If $\delta \ll 2kT$, we obtain the familiar result displaying the temperature dependence of the direct process,

$$T_{1d}^{-1} \approx 2KkT/\delta \equiv AT. \tag{6}$$

The solution of Eq. (5c) is $n(t) = n_0 + [n(0) - n_0] \times \exp(-t/T_{1d})$. Since paramagnetic resonance absorption signals are proportional to n, one may thus measure T_{1d} simply by observing the exponential recovery of the signal after making $n(0) \approx 0$ by a saturating pulse.

Turning now to the question of the evaluation of A in (7), we note that a proper but formidable approach would be the normal mode analysis of Van Vleck. However, Orbach[10] has pointed out that the rare earth ions lend themselves nicely to a simpler approach which may yield estimates of A to within an order of magnitude or better—and it is this procedure that we briefly review here and use in Sec. IV. The point of departure is the theory of Elliott and Stevens[16-19] for the ethyl sulfates and of Judd[20,21] for the double nitrates, wherein one writes the static crystal field interaction for the rare earth ion as an expansion in normalized spherical harmonics

$$\mathfrak{K}_c = \sum_{nm} V_n^m = \sum_{\substack{n=2,4,6 \\ -n \le m \le n}} B_n^m r^n Y_n^m(\theta, \varphi). \tag{8}$$

This is often rewritten in rectangular coordinates as $\mathfrak{K}_c = \sum_{nm} A_n^m G_n^m(x,y,z)$, where the G_n^m are unnormalized Legendre polynomials. Now the relaxation perturbation $\mathfrak{K}_c'$ is just the fluctuation in $\mathfrak{K}_c$, due to thermal lattice strains ϵ, and may be treated very similarly. Let ξ represent the coordinate of a ligand and expand $B_n^m(\xi)$ in a Taylor's series

$$B_n^m(\xi) = B_n^m(\xi_0) + \epsilon \xi \left(\frac{\partial B_n^m}{\partial \xi} \right)_0$$
$$+ \frac{1}{2} \epsilon \epsilon' \xi \xi' \left(\frac{\partial^2 B_n^m}{\partial \xi \partial \xi'} \right)_0 + \cdots. \tag{9}$$

The term linear in ϵ (which, as Van Vleck[3] points out, must be retained in our Hamiltonian) will give rise to one phonon, or direct processes. If we make the reasonable assumption that B_n^m is proportional to some inverse power of ξ, then we can make the approximation that

$$|b_n^m| \equiv |\xi(\partial B_n^m/\partial \xi)_0| \approx |B_n^m(\xi_0)|, \tag{10}$$

which is just the static term, usually known experimentally. Thus, the relaxation perturbation is approximately given in form and magnitude, for the direct process, by

$$\mathfrak{K}_c' \approx \epsilon \sum_{nm} b_n^m r^n Y_n^m(\theta, \varphi) \equiv \epsilon \sum_{nm} v_n^m, \tag{11}$$

where ϵ is an average thermal strain, randomly fluctuating in time.

From first-order time-dependent perturbation theory we calculate the transition probability per second for a transition of the combined spin-phonon system from the initial state $[|b\rangle, \bar{p}_0(\delta)]$ to the final state $[|a\rangle, \bar{p}_0(\delta) + 1]$:

$$w_{b \to a} = (2\pi/\hbar)\rho(\delta) |\langle \bar{p}_0(\delta) | \epsilon | \bar{p}_0(\delta) + 1 \rangle|^2$$
$$\times |\langle b | \sum_{nm} v_n^m | a \rangle|^2 \sec^{-1}. \tag{12}$$

The square of the matrix element of the strain ϵ is[15] $\delta[\bar{p}_0(\delta) + 1]/2Mv^2$, where M is the mass of the crystal. The matrix elements of v_n^m may be evaluated by the operator equivalent method[16] in exact analogy to the static terms $V_n^m = A_n^m G_n^m(x,y,z)$. The relation is[18]

$$\langle J, J_z + m | v_n^m | J, J_z \rangle$$
$$= a_n^m \langle r^n \rangle \chi_n \langle J, J_z + m | o_n^m | J, J_z \rangle, \quad -n \le m \le n. \tag{13}$$

The χ_n are operator equivalent factors and are equal to the α, β, and γ given by Stevens[16] for $n = 2, 4$, and 6, respectively. The o_n^m are operators in $J_{\pm}$, J_z and are defined by $o_n^{+m} + o_n^{-m} = O_n^m$, $m > 0$; $o_n^0 = O_n^0$. The O_n^m are the operators as usually defined in the literature.[22] For example,

$$O_2^1 = \frac{1}{4}[J_z(J_+ + J_-) + (J_+ + J_-)J_z], \tag{14a}$$

$$o_2^{+1} = \frac{1}{4}[J_z J_+ + J_+ J_z], \tag{14b}$$

$$o_2^{-1} = \frac{1}{4}[J_z J_- + J_- J_z]. \tag{14c}$$

The a_n^m are related to the b_n^m in (11) by normalizing factors. For the C_{3h} symmetry of the ethyl sulfate the only nonvanishing static terms are B_2^0, B_4^0, B_6^0, and B_6^6; for the C_{3v} symmetry of the double nitrate the additional terms are B_4^3 and B_6^3. Orbach has analyzed the lattice vibrational modes and finds that all of the b_n^m are nonvanishing. However, Judd[23] has noted that for the known values of the B_n^m (reduced from optical absorption and paramagnetic resonance data) a good empirical rule is $|B_n^m| \approx |B_n^0|$. Using Eq. (10), we thus

[16] K. W. H. Stevens, Proc. Phys. Soc. (London) A65, 209 (1952).
[17] R. J. Elliott and K. W. H. Stevens, Proc. Roy. Soc. (London) A215, 437 (1952).
[18] R. J. Elliott and K. W. H. Stevens, Proc. Roy. Soc. (London) A218, 553 (1953).
[19] R. J. Elliott and K. W. H. Stevens, Proc. Roy. Soc. (London) A219, 387 (1953).
[20] B. R. Judd, Proc. Roy. Soc. (London) A227, 552 (1955).
[21] B. R. Judd, Proc. Roy. Soc. (London) A232, 458 (1955).
[22] J. M. Baker, B. Bleaney, and W. Hayes, Proc. Roy. Soc. (London) A247, 141 (1958).
[23] B. R. Judd (private communication).

arrive at the rule $|b_n^m| \approx |B_n^0|$ to be used for estimating the many b_n^m from the few known static values. Actually, the required parameters in Eq. (13) are the $a_n^m \langle r^n \rangle$, given by

$$|a_n^m \langle r^n \rangle| \approx g_n^{|m|} |A_n^0 \langle r^n \rangle|_{\text{exp}}, \quad (15)$$

where the $g_n^{|m|}$, listed in Table I, are certain normalizing factors relating $r^n Y_n^m(\theta, \varphi)$ and $G_n^m(x,y,z)$, and the $|A_n^0 \langle r^n \rangle|_{\text{exp}}$ are the measured static values in Judd's notation.[21]

In this approximation the signs of the a_n^m are unknown and, since many of the matrix elements turn out to be of comparable magnitude, the evaluation of $|\langle b | \sum v_n^m | a \rangle|^2$ raises the question of the coherence of the different terms. By considering the time incoherence of the various lattice modes and the distribution of the thermal strain directions, we conclude that the best approximation is to consider each term $v_2^0, v_2^{+1}, v_2^{-1}, \cdots$, incoherent. To be explicit, we take

$$|\langle b | \sum_{nm} v_n^m | a \rangle|^2 = \sum_{nm} |\langle a | v_n^m | b \rangle|^2$$

$$= \sum_{\substack{n=2,4,6 \\ -n \leq m \leq n}} |X_n g_n^{|m|} |A_n^0 \langle r^n \rangle| |_{\text{exp}} \langle a | o_n^m | b \rangle|^2. \quad (16)$$

From Eqs. (3a), (7), (12), and (13) we finally obtain the expression

$$\frac{1}{T_{1d}} = \frac{3}{2\pi \rho v^5 \hbar} \left(\frac{\delta}{\hbar}\right)^3 \sum_{nm} |\langle a | v_n^m | b \rangle|^2 \frac{2kT}{\delta} \equiv AT, \quad (17)$$

for the spin-lattice relaxation rate between $|a\rangle$ and $|b\rangle$, where $\rho = M/V$ is the crystal density. If the states are a non-Kramers doublet, it is sufficient to use for $|a\rangle$ and $|b\rangle$ the zero-order wave functions, i.e., the eigenfunctions of $\mathcal{3C}_c$.

However, if $|a\rangle$ and $|b\rangle$ are a Kramers doublet, the matrix elements in (17) vanish in zero order and one must take account of the admixing of $|a\rangle$ and $|b\rangle$ with $|c\rangle$ and $|d\rangle$ (in Fig. 1) by the Zeeman perturbation $\mathcal{3C}_z = \Lambda \beta \mathbf{H} \cdot \mathbf{J}$. The relaxation rate in this case becomes

$$\frac{1}{T_{1d}} = \frac{3}{2\pi \rho v^5 \hbar} \left(\frac{\delta}{\hbar}\right)^3 \left(\frac{2\beta \Lambda}{\Delta_1}\right)^2 \sum_{nm} |\langle a | \mathbf{H} \cdot \mathbf{J} | c \rangle \langle c | v_n^m | b \rangle$$

$$+ \langle a | v_n^m | c \rangle \langle c | \mathbf{H} \cdot \mathbf{J} | b \rangle|^2 (2kT/\delta) \equiv A'T. \quad (18)$$

It may be necessary to include similar terms for $|e\rangle$ and $|f\rangle$, etc.

B. The Orbach Process

In cases where the crystal field splitting Δ_1 (ergs) is less than the maximum phonon energy $k\Theta$ ($\Theta = $ Debye temperature $\approx 60°$K for our crystals), then relaxation between $|a\rangle$ and $|b\rangle$ may proceed by the two-stage process invoked by Finn, Orbach, and Wolf[11] and later

TABLE I. Values of the normalizing factors $g_n^{|m|}$ of Eq. (15).

$|m| = $	1	2	3	4	5	6
$n=2$	4.90	2.45				
$n=4$	8.95	6.32	23.6	8.37		
$n=6$	12.9	10.2	20.2	11.2	52.7	15.2

treated in detail.[10] Throughout this paper we refer to this as the Orbach process to distinguish it from the higher order two-phonon Raman process of Sec. II C. We note that the Orbach process is very closely related to the *statistical* process of second order introduced some time ago by Lloyd and Pake.[12]

Consider a three-level spin system $|a\rangle$, $|b\rangle$, $|c\rangle$ of Fig. 1, ignoring $|d\rangle$, $|e\rangle$, $|f\rangle$. It is possible for the relaxation perturbation $\mathcal{3C}_c'$ to induce a spin flip from $|b\rangle$ to $|c\rangle$ simultaneously with the absorption of a phonon of energy Δ_1, thus conserving energy. The transition probabilities for this, and its reverse, are

$$w_{b \to c} = B_1 \bar{p}_0(\Delta_1) \text{ sec}^{-1}, \quad (19a)$$

$$w_{c \to b} = B_1 [\bar{p}_0(\Delta_1) + 1] \text{ sec}^{-1}, \quad (19b)$$

where $\bar{p}_0(\Delta_1)$ is the average phonon excitation number at energy Δ_1. Then, after a short while, there may be a spin flip from $|c\rangle$ to $|a\rangle$ and the creation of a phonon of energy $\Delta_1 + \delta$, with the transition probability

$$w_{c \to a} = B_2 [\bar{p}_0(\Delta_1 + \delta) + 1] \text{ sec}^{-1}, \quad (20a)$$

and

$$w_{a \to c} = B_2 \bar{p}_0(\Delta_1 + \delta). \quad (20b)$$

Taking $B_1 \approx B_2 = B$,[23a] and neglecting any true direct process $w_{a \leftrightarrow b}$, we write the rate equations

$$\dot{N}_b = B\{N_c [\bar{p}_0(\Delta_1) + 1] - N_b \bar{p}_0(\Delta_1)\}, \quad (21a)$$

$$\dot{N}_a = B\{N_c [\bar{p}_0(\Delta_1 + \delta) + 1] - N_a \bar{p}_0(\Delta_1 + \delta)\}. \quad (21b)$$

If $kT \ll \Delta_1$, then N_c is negligible compared to N_a and N_b. We further assume $\delta \ll \Delta_1$ and thus obtain from (21), $\dot{n} = -T_{10}^{-1}(n - n_0)$, where $T_{10}^{-1} = B \bar{p}_0(\Delta_1) \approx B \exp(-\Delta_1/kT)$. Now B may be evaluated in strict analogy with the evaluation of A in Sec. II A, to yield

$$\frac{1}{T_{10}} = \frac{3}{2\pi \rho v^5 \hbar} \left(\frac{\Delta_1}{\hbar}\right)^3 \sum_{nm} |\langle a | v_n^m | c \rangle|^2 e^{-\Delta_1/kT}$$

$$\equiv B e^{-\Delta_1/kT} \quad (22a)$$

for the relaxation rate due to the Orbach process through $|c\rangle$. In cases where there is a Kramers doublet, $|c\rangle$ and $|d\rangle$, instead of a singlet then we must replace $\sum_{nm} |\langle a | v_n^m | c \rangle|^2$ by the sum

$$\sum_{nm} |\langle a | v_n^m | c \rangle|^2 + \sum_{nm} |\langle a | v_n^m | d \rangle|^2. \quad (22b)$$

[23a] *Note added in proof.*—An exact analysis yields

$$B = 2B_1 B_2 / (B_1 + B_2).$$

C. The Raman Process

This process involves the simultaneous absorption of a phonon of energy δ_1 and the emission of another of energy $\delta_2 = \delta_1 + \delta$, along with a spin flip from $|b\rangle$ to $|a\rangle$. It is of higher order than the Orbach process in the sense that it arises in second-order time-dependent perturbation theory and also in first-order time-dependent perturbation theory with a perturbation second order in the strains. Taking the latter approach we focus attention on the doublet $|a\rangle$ and $|b\rangle$ of Fig. 1, ignoring $|c\rangle$, $|d\rangle$, etc. We take the relaxation perturbation from the third term of Eq. (9)

$$\mathfrak{IC}_c'' \approx \epsilon_1 \epsilon_2 \sum_{nm} v_n{}^m. \qquad (23)$$

By first-order theory, the transition probability is

$$w_{b \to a} = \int \frac{2\pi}{\hbar} |\langle b, \bar{p}_0(\delta_1), \bar{p}_0(\delta_2)|$$

$$\times \mathfrak{IC}_c'' |a, \bar{p}_0(\delta_1)-1, \bar{p}_0(\delta_2)+1\rangle|^2 \rho(\delta_2)\rho(\delta_1)d\delta_1. \quad (24)$$

In contrast to the Orbach process where the phonon energy must equal the crystal field splitting Δ_1, the only requirement now is that the difference of the two phonon energies be $\delta_2 - \delta_1 = \delta$ for over-all energy conservation. Since $\delta \ll k\Theta$, the entire phonon spectrum is available, hence the integral in (24). The rate equation becomes

$$\dot{N}_b = \frac{9 \sum_{nm} |\langle a|v_n{}^m|b\rangle|^2}{8\rho^2 \pi^3 \hbar^7 v^{10}} \int N_a \bar{p}_0(\delta_2)[\bar{p}_0(\delta_1)+1]$$

$$- N_b \bar{p}_0(\delta_1)[\bar{p}_0(\delta_2)+1]\delta_1{}^6 d\delta_1. \quad (25)$$

If $\delta \ll kT$, $\delta \ll \delta_1$, (25) leads to the usual form $\dot{n} = -T_{1R}^{-1} \times (n - n_0)$, where

$$\frac{1}{T_{1R}} = \frac{9 \sum_{nm} |\langle a|v_n{}^m|b\rangle|^2}{4\rho^2 \pi^3 \hbar^7 v^{10}} \int_0^{k\Theta} \frac{\delta_1{}^6 e^{\delta_1/kT} d\delta_1}{(e^{\delta_1/kT}-1)^2}. \quad (26)$$

Ziman[24] gives values of this integral; however, we shall assume $\Theta \gg T$ for helium temperatures, in which case the integral has the approximate value $(kT)^7 6!$ yielding

$$\frac{1}{T_{1R}} = \frac{9 \times 6!}{4\rho^2 \pi^3 v^{10}} \left(\frac{k}{\hbar}\right)^7 \sum_{nm} |\langle a|v_n{}^m|b\rangle|^2 T^7 \equiv CT^7 \quad (27)$$

for the Raman process. It should be noted that since no higher spin states $|c\rangle$, etc. are assumed in this calculation, the result applies only to a non-Kramers doublet, for the matrix elements of $v_n{}^m$ vanish for a pure Kramers doublet. Of course, one often finds higher spin states, say $|c\rangle$ at Δ_1, which a magnetic field will admix with a ground Kramers doublet. In this case the relaxation

[24] J. M. Ziman, Proc. Roy. Soc. (London) A226, 436 (1954).

rate will be given by (27), reduced by the factor $(2\Lambda\beta H/\Delta_1)^2$. This calculation thus predicts $T_{1R}^{-1} \propto T^7$ for non-Kramers doublets and $T_{1R}^{-1} \propto H^2 T^7$ for Kramers doublets.

The existence of a higher state $|c\rangle$ allows for an additional calculation of the Raman process by second order time-dependent perturbation theory. For a non-Kramers doublet $|a\rangle$, $|b\rangle$ and a singlet $|c\rangle$ at Δ_1, the final result is an expression

$$T_{1R}^{-1} = C'' T^7 \qquad (28a)$$

obtained from (27) by replacing $\sum_{nm} |\langle a|v_n{}^m|b\rangle|^2$ by

$$\frac{1}{\Delta_1{}^2} \{ \sum_{nm} |\langle a|v_n{}^m|c\rangle|^2 \sum_{nm} |\langle c|v_n{}^m|b\rangle|^2 \}. \qquad (28b)$$

The two calculations yield rates of comparable magnitude, i.e., $C \approx C''$, and should be added together. For a ground Kramers doublet $|a\rangle$ and $|b\rangle$, and a higher doublet $|c\rangle$ and $|d\rangle$ at Δ_1, the result of the second-order calculation is

$$\frac{1}{T_{1R}} = \frac{9! \hbar^2}{\pi^3 \rho^2 v^{10} \Delta_1{}^4} \left(\frac{k}{\hbar}\right)^9 \sum_{nm} |\langle a|v_n{}^m|c\rangle|^2$$

$$\times \sum_{nm} |\langle c|v_n{}^m|b\rangle|^2 T^9 \equiv C' T^9. \quad (29)$$

The T^9 dependence arises from the fact that there is a partial "Van Vleck" cancellation (because of time-reversal symmetry) in the summing over both $|c\rangle$ and $|d\rangle$. It is easily shown that (29) dominates the rate obtained in the preceding paragraph for Kramers doublets.

To summarize Sec. II A, B, and C, we assume that all the processes add to give for the ground doublet of a rare earth ion the total spin lattice relaxation rate $T_1^{-1} = T_{1d}^{-1} + T_{1o}^{-1} + T_{1R}^{-1}$, which can be written for a Kramers doublet as

$$(T_1^{-1})_K = A'T + B \exp(-\Delta_1/kT) + C'T^9, \quad (30)$$

and for a non-Kramers doublet as

$$(T_1^{-1})_{NK} = AT + B \exp(-\Delta_1/kT) + (C+C'')T^7, \quad (31)$$

with the A, A', $\cdots$, as defined above. The direct process will be an appreciable contribution to T_1^{-1} only at the lowest temperatures (where the others become negligible), since it is proportional to the number of phonons $\bar{p}_0(\delta) \approx kT/\delta$ in a narrow band at the very low frequency end of the phonon spectrum. For Kramers doublets $T_{1d}^{-1} \propto H^4$, and for non-Kramers doublets $T_{1d}^{-1} \propto H^2$. The Orbach process, being two "high-frequency" direct processes in cascade, is proportional to the number of phonons $\bar{p}_0(\Delta_1) \approx \exp(-\Delta_1/kT)$ in a narrow band at $\Delta_1 \approx$ crystal field splitting. It is independent of H and should be important if Δ_1/k is less

than the Debye temperature Θ. The Raman process, also independent of H, is a higher order two-phonon process for which essentially the entire phonon spectrum is available, so that it may be comparable to the Orbach process, or even dominate if $\Delta_1/k \gtrsim \Theta$.

D. The Phonon Bottleneck

In Sec. II A, B, C we have been assuming that the *spins* relax to the *phonons*, which are in such excellent thermal contact with the *bath* that the phonon excitation $\bar{p}$ always maintains its thermal equilibrium value $\bar{p}_0$ at the bath temperature. The calculated spin-lattice relaxation time T_1 is, strictly speaking, the spin-phonon relaxation time. Our measurements acutally measure the spin-bath relaxation time T_b which is, of course, identical to T_1 if $\bar{p} = \bar{p}_0$. However for the direct process there are relatively few phonons available for transporting the energy from the spins to the bath; if the spin temperature is made very high by a saturating pulse, the lattice oscillators in a narrow band at δ may be excited to a higher energy state, corresponding to a phonon excitation number

$$\bar{p}(\delta) = [\exp(\delta/kT_p) - 1]^{-1}, \qquad (32)$$

where T_p is the "hot phonon" temperature; we visualize this as a narrow spike at δ on the phonon spectrum. Van Vleck[6] first discussed this possibility some years ago. It is clear that if this phenomena persists we cannot equate the measured T_b to T_{1d}. In fact, if T_{1d} is short enough, then T_b may instead be related to the phonon-bath relaxation time, a situation described as a phonon bottleneck. Several unsuccessful attempts to detect hot phonons have been reported.[8,25,26] More recently Nash[27] has observed relaxation rates in copper Tutton salts which are dependent on crystal size and may be limited by a phonon bottleneck.

We generalize the treatment in Sec. II A to take into account nonequilibrium phonons by using $\bar{p}$ of (32) instead of $\bar{p}_0$. The rate equation (4) for the spins becomes, with the value of K from (6),

$$\dot{n} = -(1/T_{1d}) \tanh(\delta/2kT)[n(2\bar{p}+1) - N], \qquad (33)$$

where $n = N_a - N_b$ and $N = N_a + N_b$. Following Faughnan and Strandberg[8] somewhat, we get a rate equation for the average phonon excitation $\bar{p}$ of the phonons in a narrow band at δ by assuming that, in the absence of the spins, $\bar{p}$ approaches $\bar{p}_0$ exponentially with a time constant $T_{\rm ph}$, the average hot phonon-bath relaxation time; we ignore spatial diffusion effects. A spin flip from $|b\rangle$ to $|a\rangle$ increases n by two units and decreases the number of phonons $\rho(\delta)\bar{p}(\delta)(\Delta\delta)$ by one unit, where $\Delta\delta = h\Delta\nu$ is the bandwidth of phonons in interaction with the spins; we will assume that $\Delta\nu$ is given approxi-

mately by the observed paramagnetic resonance linewidth. Thus, the total rate is

$$d\bar{p}/dt = \tfrac{1}{2}[(\dot{n})/(\Delta\delta)\rho(\delta)] - [(\bar{p} - \bar{p}_0)/T_{\rm ph})]. \qquad (34)$$

Equations (33) and (34) are the rate equations for the coupled spin-phonon system, and may be rewritten as

$$\dot{n} = -\frac{1}{T_{1d}}(n - n_0) - \frac{1}{T_d}\frac{n}{\bar{p}_0 + \tfrac{1}{2}}(\bar{p} - \bar{p}_0), \qquad (35a)$$

$$\frac{d\bar{p}}{dt} = -\frac{1}{\sqrt{2}_{\rm ph}}\frac{\sigma(\bar{p}_0 + \tfrac{1}{2})}{n_0}(n - n_0)$$
$$-\frac{1}{T_{\rm ph}}\left(\sigma\frac{n}{n_0} + 1\right)(\bar{p} - \bar{p}_0), \qquad (35b)$$

where $\sigma = T_{\rm ph} n_0 / 2T_{1d}(\bar{p}_0 + \tfrac{1}{2})(\Delta\delta)\cdot\rho(\delta)$ is an important parameter called the bottleneck factor. It may be written as

$$\sigma = (E_z/T_{1d})/(E_p/T_{\rm ph}), \qquad (36)$$

where $E_z = \tfrac{1}{2}\delta N \tanh(\delta/2kT)$ is the Zeeman energy of the spin system and $E_p = \tfrac{1}{2}\rho(\delta)\;\delta\;(\Delta\delta)\coth(\delta/2kT)$ is the energy of the phonon system. Thus, σ is the (energy exchange rate between spins and phonons)/(energy exchange rate between phonons and bath). If $\sigma \ll 1$, we have the condition assumed in Sec. II A; if $\sigma \gg 1$, we have a severe bottleneck.

Solutions for the nonlinear Eqs. (35a) and (35b) have been computed[8] and show nonexponential behavior of $n(t)$. Most of our measurements are made with $(n_0 - n) \ll n_0$, so that (35a) and (35b) may be approximately replaced by the linearized equations:

$$\dot{n} = \frac{1}{T_{1d}}(n - n_0) - \frac{1}{T_{1d}}\frac{n_0}{\bar{p}_0 + \tfrac{1}{2}}(\bar{p} - \bar{p}_0), \qquad (37a)$$

$$\frac{d\bar{p}}{dt} = -\frac{1}{T_{\rm ph}}\frac{\sigma(\bar{p}_0 + \tfrac{1}{2})}{n_0}(n - n_0) - \frac{1}{T_{\rm ph}}(\sigma + 1)(\bar{p} - \bar{p}_0). \qquad (37b)$$

The solutions to (37a) and (37b) display two time constants, T_b and T_b', where

$$T_b \cong T_{1d} + \tau_1,$$

$$\frac{1}{\tau_1} = \frac{1}{T_{\rm ph}}\frac{E_p}{E_z} = \frac{1}{T_{\rm ph}}\frac{3\delta^2(\Delta\delta)[\coth(\delta/2kT)]^2}{2\pi^2 cv^3\hbar^3}$$

$$\approx \frac{1}{T_{\rm ph}}\frac{6(\Delta\delta)k^2T^2}{\pi^2 cv^3\hbar^3}$$

$$\approx 6 \times 10^{12}\frac{(\Delta H)g}{T_{\rm ph}c}T^2 \equiv DT^2 \text{ sec}^{-1}, \qquad (38a)$$

$$\frac{1}{T_b'} = \frac{1}{T_{1d}}\frac{E_z}{E_p} \approx \frac{A\pi^2 cv^3\hbar^3}{6(\Delta\delta)k^2T}$$

$$\approx 1.6 \times 10^{-13}\frac{Ac}{(\Delta H)g}\frac{1}{T} \text{ sec}^{-1}, \qquad (38b)$$

[25] K. Dransfeld, Bull. Am. Phys. Soc. **3**, 324 (1958); N. S. Shiren and E. B. Tucker, Phys. Rev. Letters **2**, 206 (1959).

[26] J. G. Castle, P. F. Chester, and P. E. Wagner, Phys. Rev. **119**, 953 (1960).

[27] F. R. Nash, Phys. Rev. Letters **7**, 59 (1961).

where $c = N/V$ is the number of spins per cm³, and $\Delta H = (\Delta\delta)/g\beta =$ linewidth in Oe, and we have taken $v \approx 2.5 \times 10^5$ cm/sec in the numerical evaluation. It should be mentioned that the approximate results of (38) are based on the assumptions that $E_z \gg E_p$ and also that either $\sigma \gg 1$ or that T_{1d} and T_{ph} are very different; these are quite well justified in our cases. Although n and $\bar{p}$ each decay with the two time constants T_b and T_b', it is easily seen that the principal change in n after a pulse occurs in a time T_b. The principal change in $\bar{p}$ occurs in a much shorter time T_b'. After the signal n has almost recovered to its thermal equilibrium value n_0, then both the spins and the phonons have reached a common temperature slightly above the bath temperature, and together decay exponentially to the bath temperature with time constant T_b.

Now T_{ph} is the time for the hot phonons in a narrow band at δ to relax either to the helium bath directly, or else into other phonons of sufficiently different energy. Some possibilities are:

(a) phonon-phonon collisions, strongly temperature dependent and probably negligible at helium temperatures;

(b) scattering by impurities or defects, strongly frequency dependent and probably negligible at the low frequency $\nu = \delta/h$; however, this process is not inelastic and so cannot contribute here.

(c) direct transmission of lattice waves into bath at the crystal boundary, independent of temperature and frequency but dependent on the linear crystal dimension l approximately as $T_{ph} \approx lQ/v$, where Q is the number of boundary reflections. The acoustic mismatch between the crystal and the liquid helium yields $Q \approx 100$, typically.

(d) inelastic scattering at the crystal surfaces into other phonon energies, with $T_{ph} \approx l/v$. This may proceed by a yet uninvestigated process, originating, e.g., in a microscopically rough "lossy" surface.

Anticipating the experimental result that $T_{ph} \sim l/v$, in (38a) we write $\tau_1^{-1} = DT^2$, where D is temperature independent and proportional to $(\Delta H)/cl$. To get the order of magnitude of τ_1 and T_b' we take $\Delta H \approx 5$ Oe, $g \approx 2$, $T \approx 2°$K, $T_{ph} \approx 10^{-7}$ sec, $A \approx 10°$K^{-1} sec^{-1}, $c \approx 10^{19}$ cm^{-3}, obtaining $\tau_1 \approx 4 \times 10^{-3}$ sec, $T_b' \approx 0.6 \times 10^{-6}$ sec. The latter time will be too short to observe by our apparatus, and we only expect to observe exponential decay of n at the longer time T_b, where

$$\frac{1}{T_b} = \frac{ADT^3}{DT^2 + AT} \rightarrow AT = T_{1d}^{-1}, \quad \text{if } DT^2 \gg AT$$

$$\text{(no bottleneck)}, \quad \text{(39a)}$$

$$\rightarrow DT^2 = \tau_1^{-1}, \quad \text{if } DT^2 \ll AT$$

$$\text{(severe bottleneck)}. \quad \text{(39b)}$$

Thus, if the direct process is dominant over the Orbach

and Raman processes, and if $AT \gg DT^2$, we will not observe T_{1d}^{-1} by our method, and should replace AT and $A'T$ in (30) and (31) by DT^2, the "bottleneck processes." The bottleneck should be easily distinguishable from the direct process because of the different temperature dependence, and its dependence on ion concentration and crystal size.

Anticipating the fact that we do observe the phonon bottleneck and measure T_{ph} in Sec. IV, we solve (35a) and (35b) to get the steady-state solutions for n and $\bar{p}$ for constant excitation of the paramagnetic resonance due to a term $2W_{rf}n$ added to the right side of (35a); one finds

$$\frac{\bar{p} + \frac{1}{2}}{\bar{p}_0 + \frac{1}{2}} = \frac{T_p}{T} = \frac{1}{2}\{(1-s) + [(1+s)^2 + 4\sigma s]^{\frac{1}{2}}\}, \quad \text{(40a)}$$

$$\frac{n_0}{n} = \frac{T_s}{T} = s\sigma\left[\frac{T_p}{T} - 1\right]^{-1}, \quad \text{(40b)}$$

$$\frac{\bar{p} + \frac{1}{2}}{\bar{p}_0 + \frac{1}{2}} = \frac{1 + \sigma}{1 + \sigma(n/n_0)}, \quad \text{(40c)}$$

where $T =$ bath temperature, $T_s =$ spin temperature, $T_p =$ phonon temperature, and $s = 2W_{rf}T_{1d}$ is the usual saturation parameter. We note that for $s \rightarrow \infty$, $T_s \rightarrow \infty$ whereas $T_p \rightarrow (\sigma + 1)T$. Furthermore, for $\sigma \gg 1$, it takes much more power to half-saturate the phonons than the spins: $T_p = \frac{1}{2}(\sigma + 1)T$ for $s \approx \tau_1/T_{1d} \gg 1$, whereas $n = \frac{1}{2}n_0$ for $s \approx T_{1d}/\tau_1 \ll 1$.

Since Raman relaxation involves high-frequency phonons over a very wide bandwidth of lattice modes, it is very unlikely that a phonon bottleneck will occur. However, the Orbach process involves phonons in two narrow bands at Δ_1 and $\Delta_1 + \delta$, and could conceivably be bottle-necked, especially if Δ_1 is only a few cm^{-1}. This case can be analyzed by writing four rate equations [similar to (33) and (34)], which may be solved only approximately, to yield for the observed time constant of $n(t)$ the value $T_b'' \approx T_{10} + \tau_0$, where

$$\frac{1}{\tau_0} \approx \frac{1}{T_{ph}} \frac{6\Delta_1^2(\Delta\delta)\exp(-\Delta_1/kT)}{\pi^2\hbar^3v^3c} \equiv F\exp(-\Delta_1/kT), \quad \text{(41)}$$

where T_{ph} is now the phonon-bath relaxation time of the hot phonons at Δ_1, and may be considerably different from T_{ph} at δ, discussed above.

III. EXPERIMENTAL APPARATUS AND PROCEDURES

All of our experiments have been made on two groups of isomorphous rare earth salts, the double nitrates $X_2Mg_3(NO_3)_{12} \cdot 24H_2O$, hereafter denoted as XMN, and the ethyl sulfates $X(C_2H_5SO_4)_3 \cdot 9H_2O$, denoted XES, where X is a rare earth trivalent ion. In most cases, the paramagnetic salt is diluted with the diamagnetic lanthanum salt. Crystals are grown from a saturated

aqueous solution, usually in a desiccator at 0°C. Double nitrate crystals grown in this manner are generally clear and visually free from imperfections. Ethyl sulfate crystals, on the other hand, are often cloudy. The concentration (percentage of paramagnetic ion) quoted in Sec. IV for various crystals always refers to the concentration in the liquid from which the crystals are grown; the actual concentration in the crystals was not measured, but is presumably near the values quoted, except for Sm in LaMN. The growing solutions were prepared from 99.997% purity La and 99.9% purity X, all obtained from Lindsay Chemical Company. Normal isotopic abundances were used except as noted below for Nd. The XMN crystals grow as hexagonal plates (approximately 1 mm thick and 1 cm in diam) with the z axis perpendicular to the plate. The XES crystals are not so regular; their maximum dimension is a few mm.

X-ray analysis[28,29] shows that in XMN, the X ions are on the corners of a rhombohedron, the X-X spacing being $\sim$8.5 Å. In XES,[30] each X has two nearest neighbors at $\sim$7 Å along the z axis, and six next-nearest at $\sim$9 Å. Thus, even concentrated crystals are somewhat "magnetically" dilute; the Curie temperatures are usually less than 0.1°K. Furthermore, all X sites are magnetically equivalent in these salts.

The sample crystals were mounted in porous styrofoam plugs and inserted into the cavity of a paramagnetic resonance spectrometer. The cavity was filled with liquid helium, maintained at a temperature in the range 1.4 to 5.0°K by a pump and a monostat (for temperature stability). Temperatures were taken from the helium vapor pressure, measured with a Zimmerli gauge.

Three different resonance spectrometers were used: one operating at $\nu\sim$9 kMc/sec and fields up to 5 kOe, previously described[31]; another similar one operating in fields up to 22 kOe; and a third operating at $\nu\approx$35 kMc/sec and fields up to 22 kOe. The block diagram, Fig. 2, shows the essential details of the 9-kMc/sec apparatus. A Varian V-58 klystron, providing 0.5 watt
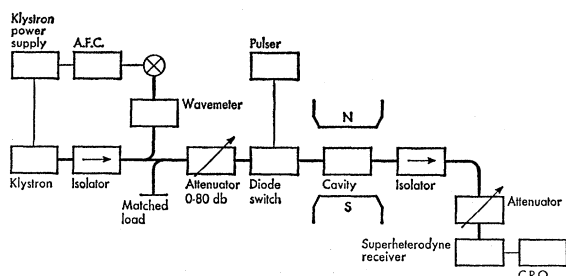

FIG. 2. Block diagram of the paramagnetic resonance spectrometer used for measuring relaxation rates at $\nu\approx$9.3 kMc/sec.

[28] A. H. Cooke, H. J. Duffus, and W. P. Wolf, Phil. Mag. 44, 623 (1953).
[29] J. W. Culvahouse, W. Unruh, and R. C. Sapp, Phys. Rev. 121, 1370 (1961).
[30] A. A. J. Ketelaar, Physica 4, 619 (1937).
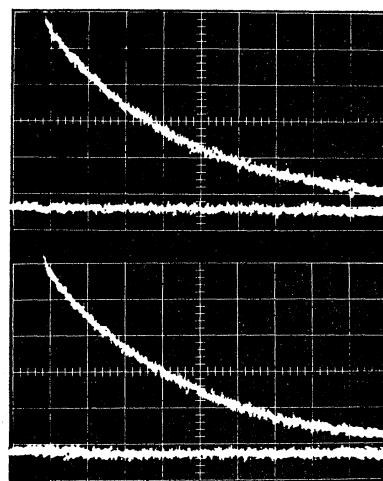[31] O. S. Leifson and C. D. Jeffries, Phys. Rev. 122, 1781 (1961).

FIG. 3. Photographs of oscilloscope trace showing transient recovery of a spin resonance signal (0.5% Nd in LaES at 4.6°K) after saturation by a pulse. The ordinate is proportional to the i.f. detector voltage, the abscissa to time (10^{-3} sec per large division). The base line gives the final thermal equilibrium signal and is drawn by triggering the oscilloscope (but not the microwave switch) at a later time.

of continuous wave power, is connected via a microwave switch to the sample cavity and thence to the detector, an APS/19 radar superheterodyne receiver capable of detecting 10^{-12} W. The i.f. output of the receiver is diode detected and fed directly into a Tektronix type 535 oscilloscope. The over-all response time of the system is $\sim10^{-6}$ sec, limited by the i.f. bandwidth. The microwave switch,[32] a simplified version of that of Feldman and McAvoy,[33] consists of two 1N419 diodes mounted across the waveguide $\frac{3}{4}\lambda$ apart. With a diode dc bias of a few volts, it is possible to set the switch for an attenuation of up to 80 db, so that the paramagnetic resonance may be observed at a sufficiently low "monitoring" power level (10^{-8} to 10^{-6} W); the receiver signal is proportional to $n=n_0$, Eq. (5b). Then, upon application of a pulse to the switch diodes the attenuation is reduced to $\approx$2 db for a pulse duration $10^{-1}>\tau>10^{-6}$ sec; this saturates the spins: $n\rightarrow0$. The transient recovery of the signal to n_0 is observed on the oscilloscope and photographed, e.g., Fig. 3. The photograph is measured and replotted on a semilog graph, Fig. 4, to determine if the decay is exponential and, if so, to measure the time constant T_b, the spin-bath relaxation time.[33a] Decays were almost always exponential except as noted below in Sec. IV. Traces were observed for various pulse widths and pulse powers and no variation in the observed T_b was detected, within experimental error of $\sim$5%.

[32] We are indebted to N. Ford for design and construction of the switch.
[33] D. W. Feldman and B. R. McAvoy, Rev. Sci. Instr. 32, 74 (1961).
[33a] The decay was measured in the tail of the transient where $(n_0-n)\ll n_0$, i.e., after the resonance signal had almost returned to its thermal equilibrium value.
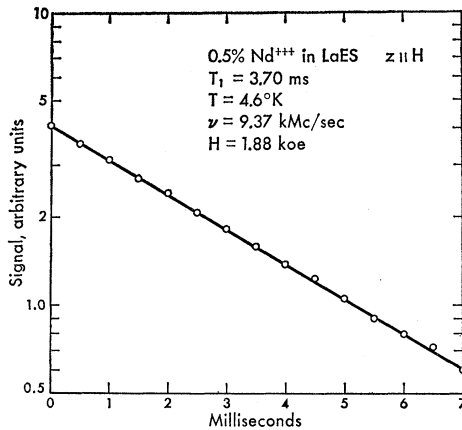
FIG. 4. A semilogarithmic plot of the traces of Fig. 3, showing the exponential form of the recovery.

The data were plotted as log T_b^{-1} vs T^{-1} (this yields a straight line for the Orbach process), and as $\log T_b^{-1}$ vs $\log T$ (this yields a straight line for the direct, Raman, or bottleneck processes). In the latter case one often has a curve of the form $T_b^{-1} = aT^m + cT^n$. The log-log plot usually determines m and n quite well. Knowing them, we then plot $T_b^{-1}T^{-m}$ vs T^{n-m}. This yields a straight line whose slope and intercept determine a and c.

The apparatus and procedure at $\nu \approx 35$ kMc/sec was quite similar to that at 9 kMc/sec. The klystron was a 10-W Elliott type 8TFK9; video detection was used instead of superheterodyne detection. The switch used a single 1N270 diode across the waveguide, giving a minimum insertion loss of ~ 15 db and an attenuation of ~ 30 db.

In addition to the bottleneck, there are several other complications in this (and other) measurements of T_1:

(a) In ions with more than two magnetic levels in the ground state, there will be a (different) rate T_1^{-1} for each pair of levels; the observed population difference n of any pair will show a transient response which includes all the rates. We have avoided this by taking ions with effective spin $S' = \frac{1}{2}$.

(b) Cross relaxation,[5] i.e., multiple spin flips not involving phonons, may occur in multilevel systems, e.g., those with hyperfine structure. This gives non-exponential decays and is temperature independent. We try to void this effect by using mostly isotopes with $I = 0$.

(c) Even for ions with a single resonance line, spin temperature transfer within the inhomogeneous components of the line may occur at a slow enough rate that one observes spectral diffusion times[34,35] instead of spin-bath relaxation times. However, the independence of our values of T_b on pulse width and power, and the exponential decays lead us to believe that we are

essentially observing the true spin-lattice relaxation rate, except for instances of phonon bottlenecking.

IV. EXPERIMENTAL RESULTS AND THEORETICAL ESTIMATES OF T_1

A. Nd in the Double Nitrate

Paramagnetic resonance of Nd in LaMN was first observed by Cooke and Duffus[36]; Judd[31] has given the theory. The spectrum consists of a strong central line due to even-even isotopes, flanked by 16 well resolved hfs lines each of about 1.2% the intensity of the central line due to the odd isotopes of natural abundance. All relaxation time measurements were made on the center of the central line with the crystal z axis perpendicular to H.

Figure 5 shows the results at $\nu = 9.37$ kMc/sec and $H = 2.48$ kOe for two different LaMN crystals, the first containing 5% Nd of natural abundance, the second containing 1% Nd enriched to 98.5% even isotopes. For both crystals the data in the range $1.4 < T < 4.2°$K are very well fitted by the expression

$$T_b^{-1} = 1.7T + 6.3 \times 10^9 \exp(-47.6/T) \text{ sec}^{-1}, \quad (42)$$

which we interpret as representing the true relaxation rate T_1^{-1} for a direct process plus an Orbach process. The value 47.6°K in the exponent is chosen to agree exactly with the optically measured field splitting for NdMN. Our relaxation data are precise enough to verify this value to $\pm 1°$K for the dilute crystals. The results are concentration independent, and cross relaxation
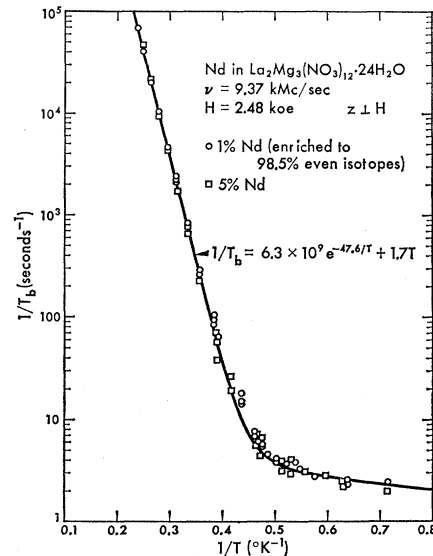

FIG. 5. The observed relaxation rate T_b^{-1} on a logarithmic scale vs reciprocal temperature T^{-1} for 1% Nd and 5% Nd in LaMN, showing clear evidence of relaxation by the Orbach process at the higher temperatures and by the direct process at the lower temperatures.

[34] K. D. Bowers and W. B. Mimms, Phys. Rev. 115, 285 (1959).
[35] W. B. Mimms, K. Nassau, and J. D. McGee, Phys. Rev. 123, 2059 (1961).
[36] A. H. Cooke and H. J. Duffus, Proc. Roy. Soc. (London) A229, 407 (1955).

effects involving hfs lines seem to be negligible. In the following paper[13] the measurements are extended down to 0.3°K where the direct process is very well displayed.

An early run on a crystal of concentrated NdMN yielded for the Orbach process

$$T_o^{-1} = 2.1 \times 10^9 \exp(-47.6/T). \quad (43)$$

We do not consider the discrepancy between (42) and (43) significant. Several runs on a given crystal always gave very reproducible data, but two different crystals (even from the same batch of growing solution) gave values of T_b^{-1} sometimes differing by a factor two or so. Our data for the Orbach process are in substantial agreement with that of Cowan, Kaplan and Browne,[37] $T_{10}^{-1} \approx 2 \times 10^9 \exp(-46 \pm 2/T)$ sec^{-1}, obtained by a microwave spin echo method on a crystal of 0.2% Nd in LaMN.

We now calculate T_{1d}^{-1} and T_{10}^{-1} from (18) and (22) and compare to the measurements. The ground state of the trivalent Nd ion is $4f^3$, $^4I_{9/2}$, which is split by the crystal field into five Kramers doublets, as shown in Fig. 6. This figure, and others which follow for other ions, is constructed rather roughly using first order perturbation theory, measured splittings and the known static field parameters $A_n^m\langle r^n\rangle$. It is shown only to give a general idea of the energy level scheme and is approximate. In the figure the crystal field levels are labelled according to the irreducible representations of the icosahedral and C_{3v} symmetry groups, using Judd's notation.[38] The two lowest γ_6 levels correspond to $|a\rangle$ and $|b\rangle$ of Fig. 1, and the lowest $(\gamma_4+\gamma_5)$ level corresponds to $|c\rangle$ and $|d\rangle$, which are degenerate in the present case where $z \perp H$. The splitting $\Delta_1/hc = 33.1$ cm^{-1} has been determined[39,40] by optical absorption. Since $\Delta_1/k = 47.6$°K is smaller than the Debye temperature $\Theta \approx 60$°K, an Orbach process is possible. In our approximate calculations we omit admixtures from the $^4I_{11/2}$ level and, for $z \perp H$, use the following wave functions[21] for $|a\rangle$ and $|b\rangle$ in terms of $|J_z\rangle$, the value $J = 9/2$ being assumed throughout.

$$|a\rangle = 0.36(|-5/2\rangle - |5/2\rangle)$$
$$+0.61(|1/2\rangle + |-1/2\rangle), \quad (44a)$$

$$|b\rangle = 0.36(|-5/2\rangle + |5/2\rangle)$$
$$+0.61(|1/2\rangle - |-1/2\rangle). \quad (44b)$$

The coefficients have been adjusted to give a best fit to the measured g gactors: the calculated values are $g_\perp = 2\Lambda\langle a|J_x|a\rangle = 2.67$ and $g_{||} = 2\Lambda\langle a|J_z|b\rangle = 0.36$, to be

[37] J. A. Cowen, D. E. Kaplan, and M. E. Browne, Proceedings of International Conference on Magnetism and Crystallography, Kyoto, Japan, 1961 (to be published).
[38] B. R. Judd, Proc. Roy. Soc. (London) **A241**, 122 (1957).
[39] H. Ewald, Ann. Physik **34**, 209 (1939).
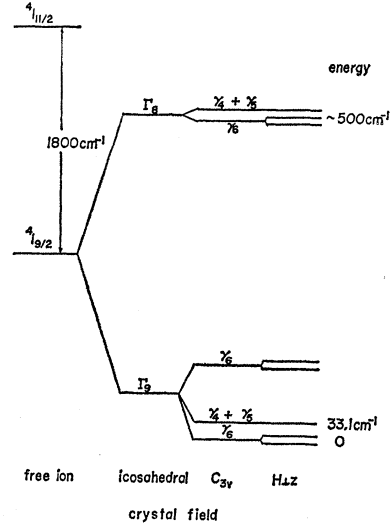[40] G. H. Dieke and L. Heroux, Phys. Rev. **103**, 1227 (1956).

FIG. 6. Splitting of the ground state $^4I_{9/2}$ of the Nd^{3+} ion in the double-nitrate crystal field. Relaxation measurements are made on the lowest Kramers doublet γ_6, which is split into $|a\rangle$ and $|b\rangle$ by a field $H \perp z$.

compared to the measured[41] values $g_\perp = 2.702 \pm 0.006$ and $g_{||} = 0.362 \pm 0.01$.

For the next higher Kramers doublet we use wave functions calculated assuming icosahedral symmetry[42]:

$$|c\rangle = -(4/9)^{\frac{1}{2}}|9/2\rangle + (7/15)^{\frac{1}{2}}|3/2\rangle$$
$$+(4/45)^{\frac{1}{2}}|-9/2\rangle, \quad (45a)$$

$$|d\rangle = (4/5)^{\frac{1}{2}}|-9/2\rangle + (7/15)^{\frac{1}{2}}|-3/2\rangle$$
$$+(4/45)^{\frac{1}{2}}|9/2\rangle. \quad (45b)$$

They yield a calculated $g_{||} = 4.2$, $g_\perp = 0$ as compared to the measured[40] values $g_{||} = 3.4$, $g_\perp = 0$; the problem of finding more exact wave functions from the present data seems underdetermined.

In calculating T_{10}^{-1} we require $\sum_{nm}|\langle a|v_n^m|c\rangle|^2$ and $\sum_{nm}|\langle a|x_n^m|d\rangle|^2$, which are equal in this case, but this is not generally true. In evaluating these we make use of Eq. (16), taking from Judd[21] $|A_2^0\langle r^2\rangle|_{\exp} = 150$ cm^{-1}, $|A_4^0\langle r^2\rangle|_{\exp} = 30$ cm^{-1}, and $|A_6^0\langle r^6\rangle|_{\exp} = 40$ cm^{-1}; and $\chi_2 = \alpha = -6.43 \times 10^{-3}$, $\chi_4 = \beta = -2.91 \times 10^{-4}$, $\chi_6 = \gamma = -3.80 \times 10^{-5}$ from Stevens.[16] Most of the matrix elements $\langle m_1|o_n^m|m_2\rangle$ required may be found from tables of matrix elements of O_n^m collected from various sources by Low[43] for $n = 2, 4, 6$ and $m = 0, 3, 4, 6$, and from tables by Jones, et al.,[44] for $m = 2$; the others ($m = 1, 5$) are readily calculated from the relevant operators, explicitly given by Orbach.[10] Some useful

[41] H. J. Stapleton (private communication); these values are more recent and are in reasonable agreement with the older values of reference 36.
[42] We are indebted to Dr. B. R. Judd for these wave functions.
[43] W. Low, *Paramagnetic Resonance in Solids* (Academic Press Inc., New York, 1960).
[44] D. A. Jones, J. M. Baker, and D. F. D. Pope, Proc. Phys. Soc. (London) **74**, 249 (1959).

relations are

$$\langle m_2 | o_n^{-m} | m_1 \rangle = \langle m_1 | o_n^{+m} | m_2 \rangle, \qquad (46a)$$

$$\langle -m_2 | o_n^{+m} | -m_1 \rangle = (-1)^m \langle m_1 | o_n^{+m} | m_2 \rangle, \quad (46b)$$

$$| \langle a | o_n^{\mp m} | d \rangle | = | \langle b | o_n^{\pm m} | c \rangle |, \qquad (46c)$$

$$| \langle a | o_n^{\mp m} | c \rangle | = | \langle b | o_n^{\pm m} | d \rangle |. \qquad (46d)$$

As an example, we calculate

$$| \langle a | v_6^{-2} | c \rangle |$$
$$= g_6^2 | A_6^0 \langle r^6 \rangle |_{\exp \gamma} | \{0.36(4/9)^{\frac{1}{2}}\langle 5/2 | o_6^{-2} | 9/2 \rangle$$
$$+ 0.61(7/15)^{\frac{1}{2}}\langle -1/2 | o_6^{-2} | 3/2 \rangle\} | \approx 45 \text{ cm}^{-1}. \quad (47)$$

Continuing thus, we find for the sums

$$\sum_{nm} | \langle a | v_n^m | c \rangle | = \sum_{nm} | \langle a | v_n^m | d \rangle | = \sum_{nm} | \langle b | v_n^m | c \rangle |$$
$$\cong 5 \times 10^{-3} \text{ cm}^{-2} = 2 \times 10^{-29} \text{ ergs}^2. \quad (48)$$

We have included all nonvanishing terms in the sums, but it is worth noting that the largest contributions come from matrix elements for $n = 6$.

The velocity of sound in the double nitrates has not been measured; we choose $v = 2.5 \times 10^5$ cm sec^{-1} as a representative value. Taking the crystal density[45] $\rho = 2.0$ g cm^{-3}, and the splitting $\Delta_1 = 6.58 \times 10^{-15}$ ergs, we find from (22) $B \approx 2.2 \times 10^{10}$ sec^{-1}. For the direct process at $\nu = 9.37$ kMc/sec, $H = 2.48$ kOe, we take $\delta = h\nu = 6.2 \times 10^{-17}$ erg, $\Lambda = 8/11$, $p = \langle c | J_x | b \rangle = 1.57$, $q = \langle a | J_x | c \rangle = 0.45$ to find from (18) $A' \approx 2.6$ sec^{-1} deg^{-1}. For the Raman process we find from (29), $C' \approx 7.8 \times 10^{-4}$ sec^{-1} deg^{-9}. To sum up, the theoretical prediction for the relaxation rate is

$$T_1^{-1} \approx 2.6T + 2.2 \times 10^{10} \exp(-47.6/T)$$
$$+ 7.8 \times 10^{-4} T^9. \quad (49)$$
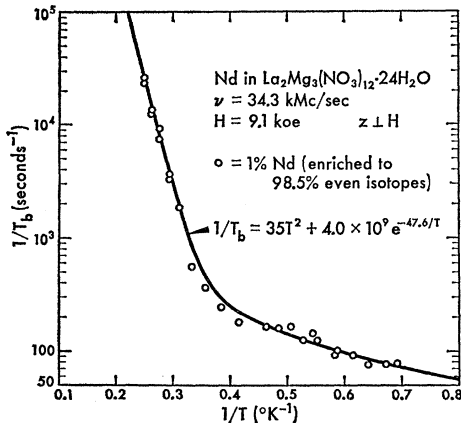
The agreement with the measurements, (42), is quite

FIG. 7. Relaxation data for 1% Nd in LaMN (the same crystal as in Fig. 5) at $H = 9.1$ kOe, showing at high temperatures an Orbach process and at lower temperatures a direct process limited by the phonon bottleneck, resulting in an observed relaxation rate T_b^{-1} proportional to T^2.

[45] C. A. Bailey, Phil. Mag. 4, 833 (1959).

acceptable, considering the many approximations in the theory; the Raman term is at least an order of magnitude smaller than the others and is not observable with our experimental uncertainty ($\sim 5\%$).

Since we have not observed a phonon bottleneck in this case, we estimate a lower limit for DT^2 in (38a) for the 1% crystal (thickness $l = 0.16$ cm) by taking $\Delta H = 4$ Oe = observed peak to peak linewidth, $g = g_\perp = 2.7$, $c = 1.6 \times 10^{19}$ = number of Nd ions per cm^3 for a 1% concentration, and $T_{\rm ph} \cong 0.3 \times 10^{-6}$ sec = time for sound waves to travel half the crystal thickness. The result is $D \approx 13$. Thus, $DT^2 \gg AT$ and we would not expect a bottleneck.

In order to check the field dependence of T_1^{-1} we also made measurements on the same 1% crystal at $H = 9.1$ kOe, $\nu = 34.3$ kMc/sec, where one expects the Orbach relaxation rate to be the same as in Fig. 6, but the direct process rate to be increased to $1.7T[9.1/2.48]^4 \approx 300T$ sec^{-1}. The results are shown in Fig. 7. The data fit reasonably well the expression

$$T_b^{-1} = 32T^2 + 4 \times 10^9 \exp(-47.6/T) \text{ sec}^{-1}. \quad (50)$$

The Orbach rate is essentially the same, as expected, but a direct process term $\propto T$ is absent; instead we observe a term $\propto T^2$, which we interpret as a phonon bottleneck. If we estimate D as in the previous paragraph, but use $\Delta H = 6.5$ Oe = measured linewidth at $H \approx 9.1$ kOe, we find $DT^2 = 21T^2$. However, $T_{1d}^{-1} = 300T = AT$ is now much larger than at 2.48 kOe and the inequality is reversed: $DT^2 \ll AT$. Thus, we now *expect* to observe the bottleneck. In fact, the observed value of $D = 32$ when compared to the predicted value $D \approx 21$ shows that our model is not far from incorrect. In particular, our assumption that

$$T_{\rm ph} \approx (\text{crystal half-thickness})/$$
$$(\text{velocity of sound}) = l/2v \quad (51)$$

seems verified. The mechanism by which the hot phonons are cooled is not clear. The crystals are not polished and may be coated with a thin crystallite layer (since they are very soluble in water), rough compared to acoustic wavelengths ($\sim 10^{-5}$ cm), so that multiple diffuse reflections among the crystallites at the boundary may allow the hot phonons to escape directly into the helium bath at the first incidence.

In an experiment to check the effect of paramagnetic impurities we made measurements of T_b^{-1} of the Nd line at $\nu = 9.37$ kMc/sec on a LaMN crystal containing 1.5% Ce, and 0.2% Pr. The data fit the expression

$$T_b^{-1} = 6.2T + 7.6 \times 10^9 \exp(-47.6/T) \text{ sec}^{-1}, \quad (52)$$

showing that the direct process, at least, is sensitive to small amounts of other paramagnetic impurities, particularly if they have a faster relaxation rate (Pr is faster by $\sim 10^5$).
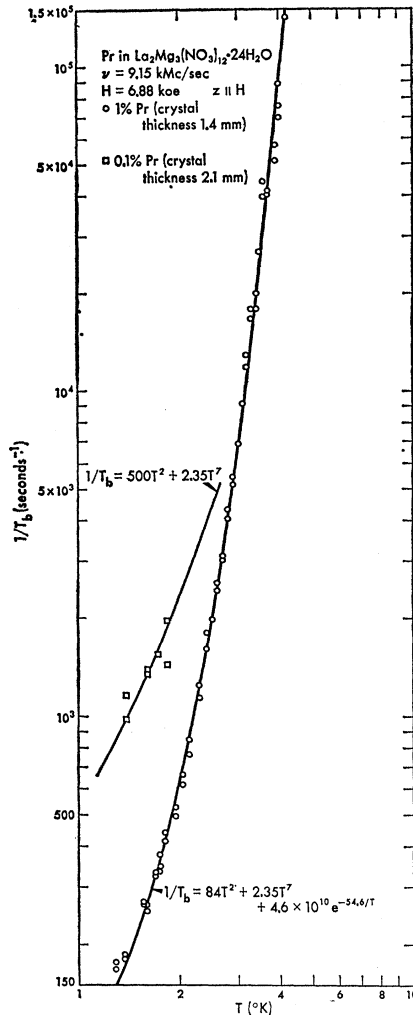
FIG. 8. Relaxation data for 1% Pr in LaMN, showing an Orbach process, a Raman process, and a direct phonon bottleneck. The additional data for 0.1% Pr in LaMN show the expected concentration and crystal size dependence of the bottleneck rate.

B. Pr in the Double Nitrate

The paramagnetic resonance spectrum[36] of Pr in LaMN consists of six well resolved hfs lines due to the 100% abundant Pr[141]. The g factors are $g_{11}=1.55$, and $g_\perp=0$; however one is still able to observe paramagnetic resonance with $H_{rf}\|H$ because of random crystal field distortions. Except as noted, all relaxation time measurements were made with $z\|H$ at $\nu=9.15$ kMc/sec on the high-field hfs line at $H=6.88$ kOe. Figure 8 gives the results for a crystal of LaMN 1.4 mm thick containing 1% Pr; the data are very well fit by the equation

$$T_b^{-1}=84T^2+4.6\times10^{10}\exp(-54.6/T)$$
$$+2.35T^7 \text{ sec}^{-1}, \quad (53)$$

which we interpret as a Raman process, plus an Orbach process, plus a direct process limited by the phonon

bottleneck. Since Pr^{3+} is a non-Kramers doublet with a fast direct relaxation rate, the bottleneck is to be expected. The Orbach term is definitely required for a fit at the higher temperatures; we have taken the value 54.6°K to agree exactly with the optical measurement and our data verify this value to ±5°K. The exponent on the Raman term is determined from the data to be 7 ± 0.5.

In order to check the expected concentration and size dependence of the bottleneck rate DT^2, data were taken for a second LaMN crystal 2.1 mm thick, containing 0.1% Pr. These results are also shown in Fig. 8 and fit the equation

$$T_b^{-1}=500T^2+2.35T^7 \text{ sec}^{-1}, \quad (54)$$

which shows that the bottleneck rate is increased over (53) by the ratio 6.0. From (51) and (38a) we note that $D\propto(lc)^{-1}$, when $l=$ thickness and $c=$ paramagnetic concentration, so that our theory would predict this ratio to be $(1.4\times1)/(2.1\times0.1)=6.7$, in good agreement with the measured value. The magnitude of D is also close to the predicted value (38a).

Our data for the Raman process are in essential agreement with Cowan et al.,[37] who find $T_{1R}^{-1}=2.8T^{6.5\pm0.5}$ sec^{-1}.

As a check to see whether cross-relaxation among the hfs levels was important, the relaxation rate $T_b^{-1}\approx DT^2$ was measured for each of the six hfs lines at $T=1.52$°K. We observed a slight decrease ($\sim20\%$) in T_b^{-1} in going from the low-field line (1.4 kOe) to the high-field line (6.9 kOe). This may qualitatively be explained by a slight decrease in the linewidth $\Delta\delta$ in (38a).

The free Pr^{3+} ion ground level $4f^2$, $^3H_4$ is split by the double nitrate crystal field into three singlets and three doublets, as in Fig. 9, and paramagnetic resonance is observed between $|a\rangle$ and $|b\rangle$ of the lowest (non-
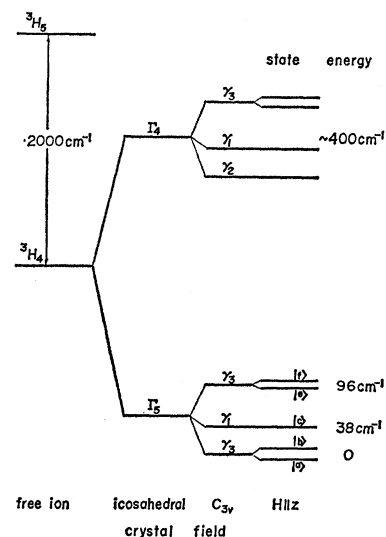

FIG. 9. Splitting of the ground state $^3H_4$ of the Pr^{3+} ion in the double nitrate crystal field. Relaxation measurements are made on the lowest magnetic doublet $|a\rangle$, $|b\rangle$.
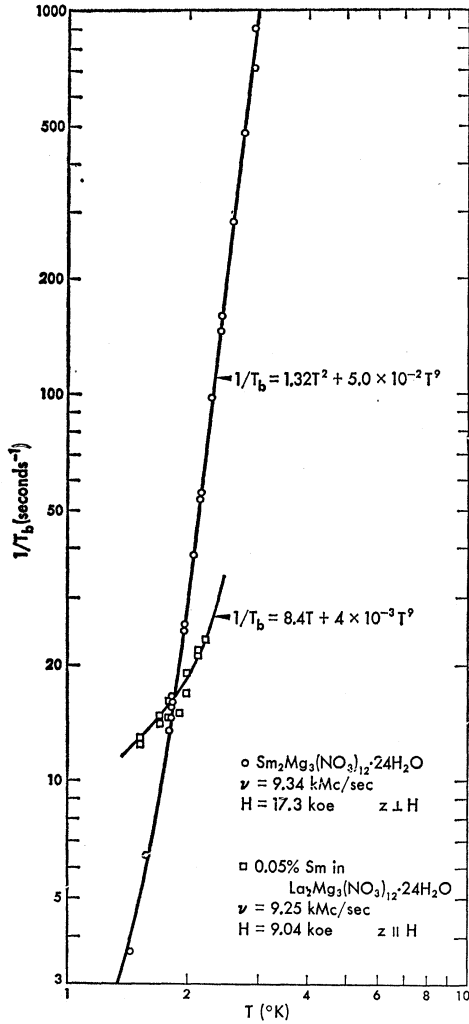
FIG. 10. Relaxation data for a crystal of SmMN, showing a Raman process at the higher temperatures and the beginning of a phonon bottleneck at the lower temperatures. Data are also shown for 0.05% Sm in LaMN, showing again a Raman process at the higher temperatures.

Kramers) doublet. The splittings $\Delta_1/hc = 38$ cm^{-1} and $\Delta_2/hc = 96$ cm^{-1} have been measured spectroscopically by Hellwege and Hellwege.[46] The wave functions for the ground doublet with $z\|H$ are,[21] in terms of $|J=4, J_z\rangle$,

$$|a\rangle = 0.458|-4\rangle + 0.756|-1\rangle + 0.467|2\rangle, \quad (55a)$$

$$|b\rangle = 0.458|4\rangle - 0.756|1\rangle + 0.467|-2\rangle. \quad (55b)$$

They yield $g_{11} = 1.56$, compared to the measured value $g_{11} = 1.55$. One calculates from Judd's[21] values of crystal field parameters,

$$|c\rangle = 0.57|3\rangle + 0.60|0\rangle - 0.57|-3\rangle, \quad (55c)$$

$$|e\rangle = 0.55|-4\rangle + 0.16|-1\rangle - 0.82|2\rangle, \quad (55d)$$

$$|f\rangle = 0.55|4\rangle - 0.16|1\rangle - 0.82|-2\rangle. \quad (55e)$$

[46] A. M. Hellwege and K. H. Hellwege, Z. Physik 135, 92 (1953).

We use the crystal field parameters $|A_2^0\langle x^2\rangle|_{exp} = 70$ cm^{-1}, $|A_4^0\langle r^4\rangle|_{exp} = 20$ cm^{-1}, $|A_6^0\langle r^6\rangle|_{exp} = 50$ cm^{-1} to calculate, as before, these sums for all nonvanishing terms:

$$\sum |\langle a|v_n^m|b\rangle|^2 = 8.7\times10^3 \text{ cm}^{-2}, \quad (56a)$$

$$\sum |\langle b|v_n^m|c\rangle|^2 = \sum|\langle c|v_n^m|a\rangle|^2 = 4.2\times10^3 \text{ cm}^{-2}, \quad (56b)$$

$$\sum |\langle b|v_n^m|e\rangle|^2 = 5.4\times10^3 \text{ cm}^{-2}, \quad (56c)$$

$$\sum |\langle b|v_n^m|f\rangle|^2 = 14.5\times10^3 \text{ cm}^{-2}. \quad (56d)$$

Terms of the type v_6^m contribute the most to these sums.

From (56a) and (17) we calculate for the direct process, $A = 7.4\times10^4$ sec^{-1} deg^{-1}. Since $\Delta_1/k = 54.6°$K is still less than Θ, we expect an Orbach process is possible for $|c\rangle$ but not for $|e\rangle$ and $|f\rangle$. From (56b) and (22a) we calculate $B = 9.7\times10^9$ sec^{-1}.

There are three terms which contribute to the Raman process: Eq. (27), using (56a); and Eqs. (28a,b) using (56b) for the level at Δ_1; and Eqs. (28a,b) using (56c) and (56d) for the levels at Δ_2. They contribute approximately equally to yield $C + C''(\Delta_1) + C''(\Delta_2) = 0.14$ sec^{-1} deg^{-7}.

Summing up, we would predict for the total spin-lattice relaxation rate:

$$T_1^{-1} = 7.4\times10^4 T + 9.7\times10^9 \exp(-54.6/T)$$
$$+ 0.14 T^7 \text{ sec}^{-1}. \quad (57)$$

The Orbach term is approximately a factor 4 less than the measured value (53), while the Raman term is a factor 16 less. An increase by a factor 2 of the dynamic field parameters v_n^m would bring both calculated terms into nearly exact agreement with the data. Such a factor is certainly within the range of approximation of the theory. We feel that the value $T_{1d}^{-1} \approx 10^5 T$ sec^{-1} is a reliable estimate of the direct process. Since T_{1d}^{-1} is much greater than the bottleneck rate DT^2 in either (53) or (54), the failure to observe the direct process is adequately explained.

C. Sm in the Double Nitrate

The paramagnetic resonance[36] spectrum of Sm in LaMN consists of a strong central line flanked by 16 well resolved hfs lines, each with 1.8% relative intensity. In the dilute salt we measure $g_\perp = 0.363\pm0.10$ and $g_{11} = 0.736\pm0.005$, in substantial agreement with the values[36] $g_\perp = 0.40$ and $g_{11} = 0.76$ for the concentrated salt. For a concentrated SmMN crystal (thickness $l = 0.9$ mm) oriented with $z\perp H$ our relaxation time measurements are shown in Fig. 10 and fit very well the expression

$$T_b^{-1} = 1.32 T^2 + 5\times10^{-2} T^9 \text{ sec}^{-1}, \quad (58)$$

displaying a direct phonon bottleneck plus a Raman process; the data determine the Raman exponent to be 9 ± 0.3. A second crystal of LaMN containing nominally 1% Sm (line intensity measurements indicated 0.05%

actual Sm concentration) was oriented $z\|H$ and some relaxation data obtained, as shown in Fig. 10, which, with some scatter, may be fit to

$$T_b^{-1} \approx 8T + 4 \times 10^{-3} T^9 \text{ sec}^{-1}. \tag{59}$$

The free ion Sm^{3+} ground state is $4f^5$, $^6H_{5/2}$ and this is split into three doublets by the crystal field; see Fig. 11. The splittings $\Delta_1/hc = 46.5$ cm^{-1} and $\Delta_2/hc = 68.9$ cm^{-1} have been measured optically by Friederich et al.,[47] and are large enough so that the Orbach process will be negligible. Although the $^6H_{5/2}$ level is seriously perturbed by the excited level $^6H_{7/2}$, we shall first make a zero-order calculation neglecting any admixtures from $J = 7/2$. Using the g factors and values of Δ_1 and Δ_2, the wave functions for $z \perp H$ in terms of $|J = 5/2, J_z\rangle$ are found to be

$$|a\rangle = 0.53(|-5/2\rangle - |5/2\rangle)$$
$$+ 0.47(|1/2\rangle + |-1/2\rangle), \tag{60a}$$

$$|b\rangle = 0.53(|-5/2\rangle + |5/2\rangle)$$
$$+ 0.47(|1/2\rangle - |-1/2\rangle), \tag{60b}$$

$$|c\rangle = |-3/2\rangle, \tag{60c}$$

$$|d\rangle = |3/2\rangle, \tag{60d}$$

$$|e\rangle = 0.47(|-5/2\rangle - |5/2\rangle)$$
$$- 0.53(|1/2\rangle + |-1/2\rangle), \tag{60e}$$

$$|f\rangle = 0.47(|-5/2\rangle + |5/2\rangle)$$
$$- 0.53(|1/2\rangle - |-1/2\rangle). \tag{60f}$$

The states $|a\rangle$ and $|b\rangle$ yield the calculated values $g_\perp = 0.382$ and $g_{\|} = 0.67$. One also deduces from this zero-order approximation the crystal field parameters: $A_2^0\langle r^2\rangle \approx -14$ cm^{-1}, $A_4^0\langle r^4\rangle \approx -15$ cm^{-1}, and $A_4^3\langle r^4\rangle \approx \pm 1440$ cm^{-1}. These are considerably different from Judd's values[21] $[A_2^0\langle r^2\rangle = -30$ cm^{-1}, $A_4^0\langle r^4\rangle = -30$ cm^{-1}, and $A_4^3\langle r^4\rangle = \mp 400$ cm$^{-1}]$ and furthermore do not obey the empirical rule $|B_n^m| \approx |B_n^0|$. Nevertheless, they are based on measured data to some extent, and we use them in estimating the sums:

$$\sum |\langle b|v_n^m|c\rangle|^2 = \sum |\langle c|v_n^m|a\rangle|^2 \approx 65 \text{ cm}^{-2}, \tag{61a}$$

$$\sum |\langle b|v_n^m|e\rangle|^2 \approx 109 \text{ cm}^{-2}, \tag{61b}$$

$$\sum |\langle e|v_n^m|a\rangle|^2 \approx 600 \text{ cm}^{-2}. \tag{61c}$$

It is noted that these sums are one or two orders of magnitude smaller than similar sums calculated for other ions in this paper. This is in part due to the absence of v_6^m terms and in part to the smallness of the $A_n^0\langle r^n\rangle$ values used. Using (61), we evaluate A' from (18), including the admixing from both $|c\rangle$, $|d\rangle$ and $|e\rangle$, $|f\rangle$, to find $A' \approx 0.2$ sec^{-1} deg^{-1}. Similarly, from (29) we find $C' \approx 1.2 \times 10^{-7}$ sec^{-1} deg^{-9}. Thus, this zero-order

[47] A. Freiderich, K. H. Hellwege, and H. Lammermann, Z. Physik 159, 524 (1960).
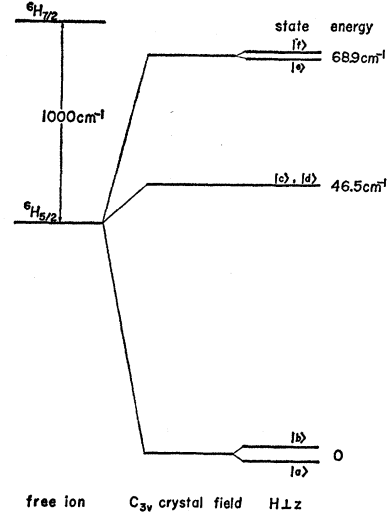
FIG. 11. Splitting of the ground state $^6H_{5/2}$ of Sm^{3+} in the double-nitrate crystal field.

calculation predicts for $z \perp H$

$$T_1^{-1} = 0.2T + 1.2 \times 10^{-7} T^9 \text{ sec}^{-1}. \tag{62a}$$

A similar calculation for $z\|H$ predicts

$$T_1^{-1} = 0.13T + 6.6 \times 10^{-8} T^9 \text{ sec}^{-1}. \tag{62b}$$

On comparison of (62) with (58) and (59) it is seen that the zero-order calculation fails miserably. The Raman process is underestimated by a factor $\sim 10^5$, and the direct process by a factor $\sim 10^2$. It seems then that the perturbation by the $^6H_{7/2}$ level must be taken into account. Judd finds that admixtures of as much as 15% of $|J = 7/2, J_z\rangle$ functions must be added into the ground state. A typical matrix element which may occur is[20]

$$\langle J = 7/2, J_z = 7/2 | v_6^3 | J = 5/2, J_z = 1/2\rangle \approx 0.1 A_6^3\langle r^6\rangle.$$

For $A_6^3\langle r^6\rangle \approx 2000$ cm^{-1}, this amounts to 200 cm^{-1}, and 15% is 30 cm^{-1}, which is larger by 10 than the largest matrix element $|\langle b|v_4^3|e\rangle| \approx 4$ cm^{-1} used in evaluating (61b). Since T_{1d}^{-1} is proportional to the second power and T_{1R}^{-1} to the fourth power of the matrix elements of v_n^m, we multiply the respective terms in (62) by, say, $(25)^2$ and $(25)^4$, respectively, to thus roughly reestimate the relaxation time

$$T_1^{-1} \approx 120T + 4.6 \times 10^{-2} T^9 \text{ sec}^{-1} \quad \text{for} \quad z \perp H, \tag{63a}$$

$$T_1^{-1} \approx 80T + 2.5 \times 10^{-2} T^9 \text{ sec}^{-1} \quad \text{for} \quad z\|H. \tag{63b}$$

The Raman terms are brought into reasonable agreement with the measurements and the observation of the phonon bottleneck for the concentrated crystal at $z \perp H$ is also clearly explained: for a linewidth $\Delta H \approx 100$ Oe, we estimate $D \approx 0.72$, so that $DT^2 \ll AT = 120T$. On the other hand, for the dilute crystal at $z\|H$, we estimate its actual concentration from signal intensity to be 0.05%, linewidth $\Delta H \approx 5$ Oe, yielding $D \approx 70$. Since

$70T^2 \gtrsim 80T$, we do not expect much of a bottleneck in this case.

D. Ce in the Ethyl Sulfate

The resonance spectrum[48] for Ce in ES consists of two lines, one each for two low-lying doublets; there is no hfs. Our measurements were made on the lowest doublet and with $z \perp H$. For a crystal of 0.2% Ce in LaMN the relaxation time measurements are shown in Fig. 12 and may be fit to the expression

$$T_b{}^{-1} = 2.2 \times 10^6 \exp(-5.67/T) \text{ sec}^{-1}, \qquad (64)$$

where the value[49] $\Delta_1/k = 5.67°K$ is verified by the relaxation measurements with an uncertainty of about 1°K. The relaxation time is much shorter than for the other ions and becomes too short to measure reliably with our apparatus above 1.8°K. Although the data are fewer and are restricted to a limited temperature range, (64) seems to indicate an Orbach process.

The free-ion ground level of Ce^{3+} is $4f^1\,{}^2F_{5/2}$, which is split by the LaES crystal field[17] into three doublets, Fig. 13, the highest of which we ignore. The splitting $\Delta_1/hc = 3.94$ cm^{-1} has been measured by microwave resonance,[49] and its smallness predicts a dominant Orbach process even at the lowest helium temperatures. For $z \perp H$, we take the wave functions in the usual notation $|J=5/2, J_z\rangle$

$$|a\rangle = 0.71(|1/2\rangle - |-1/2\rangle), \qquad (65a)$$

$$|b\rangle = 0.71(|1/2\rangle + |-1/2\rangle), \qquad (65b)$$

$$|c\rangle = 0.71(|5/2\rangle - |-5/2\rangle), \qquad (65c)$$

$$|d\rangle = 0.71(|5/2\rangle + |-5/2\rangle). \qquad (65d)$$

Equations (65a,b) yield $g_\perp = 2.60$ and $g_{||} = 0.86$ to be

FIG. 13. Splitting of the $^2F_{5/2}$ ground state of magnetically dilute Ce^{3+} in the ethyl-sulfate crystal field. Relaxation measurements are made on the lowest Kramers doublet $|a\rangle$, $|b\rangle$.

compared to the measured values[48] $g_\perp = 2.185$, $g_{||} = 0.955$. For the excited doublet Eqs. (65c,d) yield $g_\perp = 0$, $g_{||} = 4.3$, to be compared with the measured values $g_\perp = 0.20$, $g_{||} = 3.72$. We use Elliott and Stevens[17] values $|A_2{}^0\langle r^2\rangle|_{exp} = 15$ cm^{-1}, and $|A_4{}^0\langle r^4\rangle|_{exp} = 40$ cm^{-1} in calculating the sum

$$\sum|\langle a|v_n{}^m|c\rangle|^2 = \sum|\langle a|v_n{}^m|d\rangle|^2 = 2.7 \times 10^3 \text{ cm}^{-2}. \quad (66)$$

Taking the density[30] $\rho = 1.8$ g cm^{-3}, and the velocity $v \approx 2 \times 10^5$ cm sec^{-1}, we evaluate B from (22a,b) to find

$$T_1{}^{-1} = 6.9 \times 10^7 \exp(-5.67/T) \text{ sec}^{-1}, \qquad (67)$$

which is a factor 30 *greater* then the measured rate (64). Since it seems unlikely that the theoretical estimate could be in error by this much, we consider the possibility that (64) does not represent $T_1{}^{-1}$, but instead represents a phonon bottleneck of the Orbach process, as given by (41). If we take the experimental value $F = 2.2 \times 10^6$ sec^{-1} and $(\Delta\delta)/h = \Delta\nu \approx 30$ Mc/sec, we calculate $T_{ph} \approx 10^{-9}$ sec for the phonon-bath relaxation time for phonons of energy Δ_1. This is much shorter than the time required for sound waves to traverse the crystal but could possibly represent the phonon lifetime due to impurity scattering. Further experiments with various Ce concentrations are required to fully establish that (64) represents a phonon bottleneck.

E. Nd in the Ethyl Sulfate

Our relaxation time measurements have been made on the strong central line of the paramagnetic resonance spectrum[50] of Nd in LaES. With $z \perp H$, the data for 0.2% Nd (enriched to 98.5% even isotopes) in a LaES crystal at $\nu = 9.37$ kMc/sec are given in Fig. 14, and are
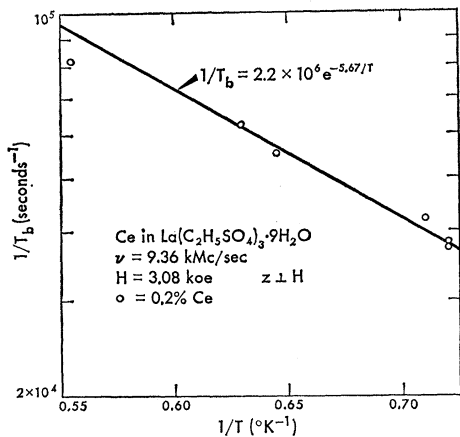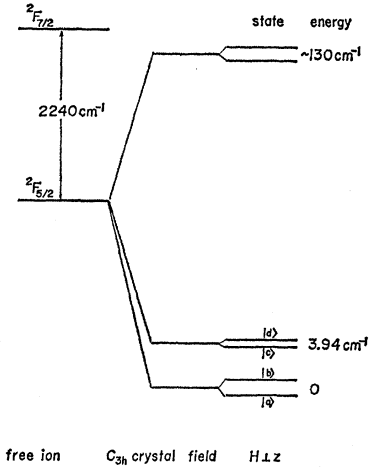

FIG. 12. Relaxation data for 0.2% Ce in LaES, showing an Orbach process which may be phonon limited.

[48] G. S. Bogle, A. H. Cooke, and S. Whitley, Proc. Phys. Soc. (London) A64, 931 (1951).

[49] D. P. Devor and R. H. Hoskins, Bull. Am. Phys. Soc. 6, 364 (1961).

[50] B. Bleaney, H. E. D. Scovil, and R. S. Trenam, Proc. Roy. Soc. (London) A223, 15 (1954).

well fit by the expression

$$T_b^{-1} = 4.4T + 3.65 \times 10^{-4}T^9 \ \text{sec}^{-1}, \tag{68}$$

clearly showing a direct process and a Raman process with exponent 9 ± 0.5. For another crystal of LaES containing 0.5% Nd, the measurements are fit by

$$T_b^{-1} = 7.6T + 3.7 \times 10^{-4}T^9 \ \text{sec}^{-1}, \tag{69}$$

while a third crystal containing 5% Nd yielded data fitted by

$$T_b^{-1} = 14.5T + 3.6 \times 10^{-4}T^9 \ \text{sec}^{-1}. \tag{70}$$

The *apparent* increase of the direct process rate with increasing Nd concentration we believe due to an increasing concentration of Ce impurity, unintentionally introduced along with the Nd. As discussed above, Ce in this salt has a much shorter relaxation time (by a factor 10^4), and through cross relaxation, could easily affect the direct process for Nd even in small concentrations.
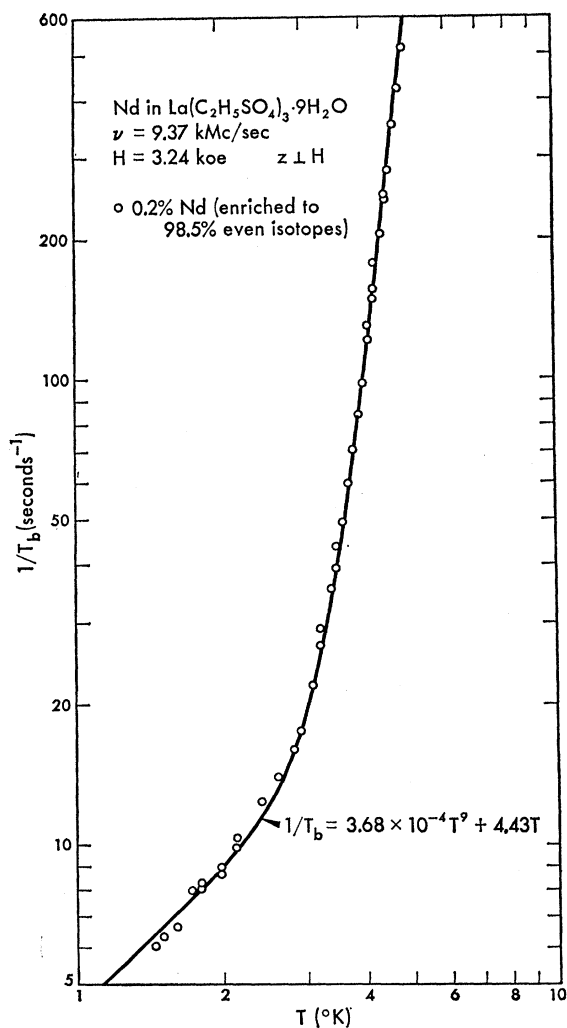

Fig. 14. Relaxation data for 0.2% Nd in LaES, clearly showing a Raman process and a direct process.
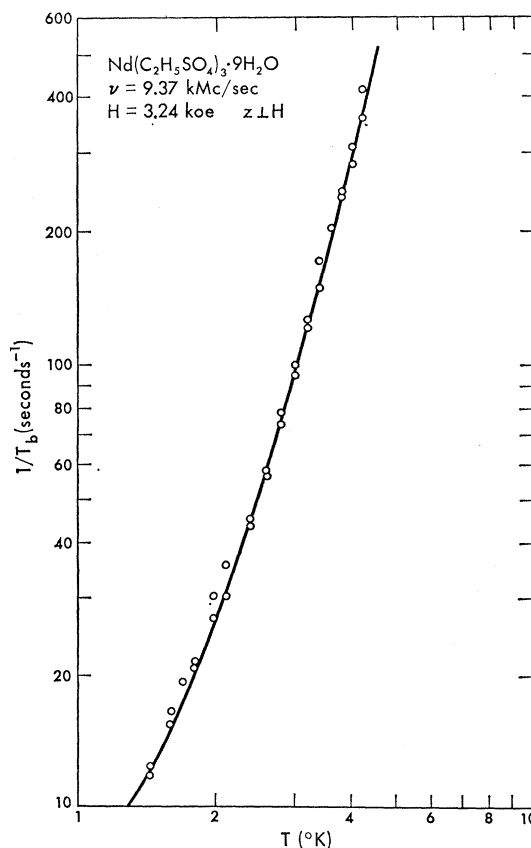

Fig. 15. Relaxation data for NdES.

Relaxation data were taken for a crystal of NdES (including probably 0.1% Ce as impurity) and are shown in Fig. 15. The relaxation times are considerably shorter than for the dilute crystals and do not fit a curve of the form $T_b^{-1} = A'T + C'T^9$, or any other reasonable form. Although Nd spin-spin interactions in the concentrated salt may be important, we feel the most likely explanation is the Ce impurity.

These cross relaxation effects were examined in more detail for a LaES crystal containing 0.5% Nd and approximately 0.001% Ce (estimated from paramagnetic resonance signal strength). The relaxation rate T_b^{-1} of Nd was measured as a function of the angle θ between the crystal z axis and the dc field H at $T = 1.4°$K, with the results of Fig. 16. At $\theta = 29.3°$ the Nd central line comes into coincidence with the line of the $|\pm 5/2\rangle$ Ce excited doublet, Eq. (65c,d); at $\theta = 78.5°$ with the $|\pm 1/2\rangle$ Ce ground doublet, Eq. (65a,b). At these points the recovery trace of the Nd signal becomes markedly nonexponential, and can be split rather well into the sum of two exponentials. Both of these rates are plotted in the figure, the fast rate probably being due to Nd ions near and in good thermal contact with Ce ions, while the slow rate may be due to more
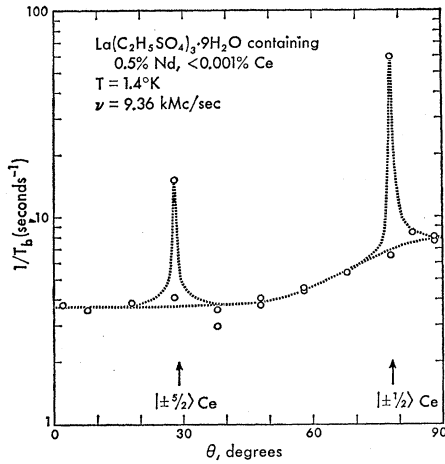
FIG. 16. Observed relaxation rate T_b^{-1} for Nd in a crystal of LaES containing also a small amount of Ce, as a function of the angle θ between crystal z axis and field H. At the angles indicated the Nd and Ce resonance lines coincide and T_b^{-1} (Nd) is considerably increased.

isolated Nd ions. The result is similar to that of Feher and Scovil[51] for Ce and Gd in LaES.

In another experiment along these lines we measured the Nd relaxation rate in a crystal of LaES containing 0.5% Nd and 0.5% Ce. It was observed that at all angles θ the Nd recovery signal was quite nonexponential. Our general conclusion is that because $T_1(Ce) \ll T_1(Nd)$, small concentrations of Ce can affect the observed Nd direct relaxation rate in the ethyl sulfate, whereas these effects are rather negligible in the double nitrate where $T_1(Ce)$ and $T_1(Nd)$ are of the same order of magnitude. By extrapolating (68), (69), and (70) to zero concentration of Nd (and also Ce) we arrive at

$$T_b^{-1} \approx 1.7T \text{ sec}^{-1} \qquad (71)$$

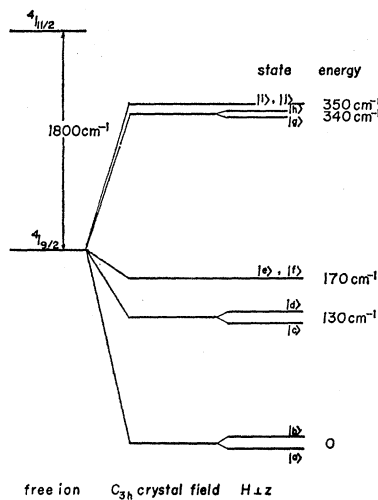as the best experimental value of the direct rate.

The ground state of the Nd ion in the LaES crystal field is split as in Fig. 17, which is constructed from the work of Elliott and Stevens.[19] We are concerned primarily with the three lower doublets, whose wave functions for $z \perp H$ are, in terms of $|J=9/2, J_z\rangle$,

$$|a\rangle = 0.65(|7/2\rangle - |-7/2\rangle)$$
$$+0.27(|-5/2\rangle - |5/2\rangle), \qquad (72a)$$

$$|b\rangle = 0.65(|7/2\rangle + |-7/2\rangle)$$
$$+0.27(|-5/2\rangle + |5/2\rangle), \qquad (72b)$$

$$|c\rangle = 0.71(|1/2\rangle - |-1/2\rangle), \qquad (72c)$$

$$|d\rangle = 0.71(|1/2 + |-1/2\rangle), \qquad (72d)$$

$$|e\rangle = 0.53(|9/2\rangle - |-9/2\rangle)$$
$$+0.47(|-3/2/\rangle - |3/2\rangle), \qquad (72e)$$

$$|f\rangle = 0.53(|9/2\rangle + |-9/2\rangle)$$
$$+0.47(|-3/2\rangle + |3/2\rangle). \qquad (72f)$$

The functions $|a\rangle$ and $|b\rangle$ yield $g_\perp = 2.0$, $g_{||} = 3.7$ to be compared to the measured values[50] $g_\perp = 2.073$, $g_{||} = 3.535$. The splitting $\Delta_1/hc = 130$ cm^{-1} is too large to allow an Orbach process. We use the values[19] $|A_2^0\langle r^2\rangle|_{\exp} = 15$ cm^{-1}, $|A_4^0\langle r^4\rangle|_{\exp} = 35$ cm^{-1}, and $|A_6^0\langle r^6\rangle|_{\exp} = 60$ cm^{-1} to calculate the sums $\sum |\langle a|v_n^m|c\rangle|^2 = 1.1 \times 10^4$ cm^{-2}, $\sum |\langle c|v_n^m|b\rangle|^2 = 5.3 \times 10^3$ cm^{-2}, $\sum |\langle a|v_n^m|e\rangle|^2 = 6.0 \times 10^3$ cm^{-2}, $\sum |\langle e|v_n^m|b\rangle|^2 = 1.2 \times 10^4$ cm^{-2}, where again the largest contribution comes from v_6^m terms. These sums in (18) and (29) yield an estimated relaxation rate

$$T_1^{-1} = 1.4T + 1.3 \times 10^{-4}T^9 \text{ sec}^{-1}, \qquad (73)$$

which is in quite good agreement with the measurements for the Raman process, Eq. (68), and the direct process, Eq. (71).

A phonon bottleneck is not observed, nor is it expected at $\nu \approx 9$ kMc/sec: for a 1% crystal an estimate

FIG. 17. Splitting of the $^4I_{9/2}$ ground state of Nd^{3+} in the ethyl-sulfate crystal sulfate field.

[51] G. Feher and H. E. D. Scovil, Phys. Rev. **105**, 760 (1957).
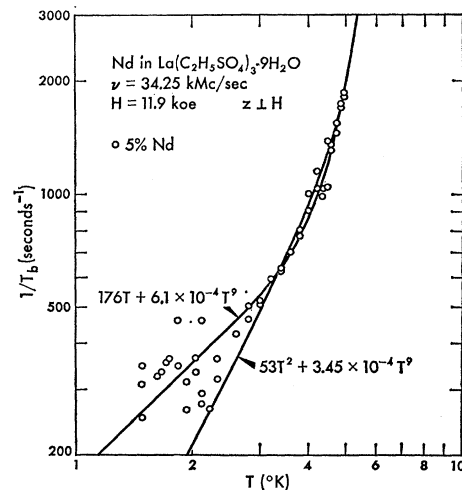

FIG. 18. Relaxation data for 5% in LaES at 11.9 kOe. The data are fit better by $T_b^{-1} = 176T + 6.1 \times 10^{-4}T^9$ sec^{-1}.

TABLE II. Comparison of measured values and theoretical estimates of the spin-lattice relaxation rates for rare ions in single crystals of the double nitrate (MN) and the ethyl sulfate (ES) in the temperature range $1.4 < T < 4.3°K$ for the direct, the Orbach and the Raman processes.

Salt		Direct T_{1d}^{-1} (in sec^{-1})	Orbach T_{1O}^{-1} (in sec^{-1})	Raman T_{1R}^{-1} (in sec^{-1})
1% Nd in LaMN $z \perp H$ $H = 2.48$ kOe	meas.[a]	$1.7T$	$6.3 \times 10^9 \exp(-47.6/T)$	
	theor.[b]	$2.6T$	$2.2 \times 10^{10} \exp(-47.6/T)$	$7.8 \times 10^{-4} T^9$
1% Pr in LaMN $z \| H$ $H = 6.8$ kOe	meas.[c]	$> 10^3 T$	$4.6 \times 10^{10} \exp(-54.6/T)$	$2.35 T^7$
	theor.[d]	$3 \times 10^5 T$	$4 \times 10^{10} \exp(-54.6/T)$	$2.2 T^7$
SmMN $z \perp H$ $H = 17.3$ kOe	meas.[e]	$> 10T$		$5 \times 10^{-2} T^9$
	theor.[f]	$120T$		$4.6 \times 10^{-2} T^9$
0.05% Sm in LaMN $z \| H$ $H = 9.04$ kOe	meas.[g]	$8T$		$4 \times 10^{-3} T^9$
	theor.[h]	$80T$		$2.5 \times 10^{-2} T^9$
1% Ce in LaES $z \perp H$ $H = 3.08$ kOe	meas.[i]		$2.2 \times 10^6 \exp(-5.6/T)$	
	theor.[j]		$6.9 \times 10^7 \exp(-5.7/T)$	
1% Nd in LaES $z \perp H$ $H = 3.24$ kOe	meas.[k]	$1.7T$		$3.6 \times 10^{-4} T^9$
	theor.[l]	$1.4T$		$1.3 \times 10^{-4} T^9$
0.2% Ce in LaMN $z \perp H$ $H = 3.75$ kOe	meas.[m]	$> 80T$	$2.7 \times 10^9 \exp(-34/T)$	
	theor.[n]	$6T$	$3.5 \times 10^9 \exp(-34/T)$	
DyES $< z, H = 45°$ $H = 1.1$ kOe	meas.[p]	$4.2T$	$1.1 \times 10^7 \exp(-23/T)$	
	theor.[q]	$6.2T$	$1.2 \times 10^7 \exp(-23/T)$	$1.3 \times 10^{-5} T^9$

[a] Equation (42). See also reference 37 and reference 53.
[b] Equation (49).
[c] Equation (53); the lower limit of T_{1d}^{-1} is estimated from the observed bottleneck. See also reference 37.
[d] Obtained from Eq. (57) by increasing $v_n{}^m$ by a factor two.
[e] Equation (58); the lower limit of T_{1d}^{-1} is estimated from the observed bottleneck.
[f] Equation (63a).
[g] Equation (59).
[h] Equation (63b).

[i] Equation (64); this value may not be the true T_{1O}^{-1}, but rather an Orbach phonon bottleneck rate.
[j] Equation (67).
[k] T_{1d}^{-1} from Eq. (71); T_{1R}^{-1} from Eqs. (68), (69), (70).
[l] Equation (73).
[m] T_{1O}^{-1} from reference 13, Eq. (5); see also reference 53. The lower limit on T_{1d}^{-1} is obtained from the measured bottleneck, reference 13, Eq. (11).
[n] T_{1d}^{-1} from reference 13, Eq. (11); T_{1O}^{-1} from reference 13, Eq. (14). See also reference 11.
[p] Reference 11.
[q] Reference 10.

of D from (38a) with linewidth $\Delta H = 10$ Oe and $T_{ph} \approx 0.2$ 10^{-6} sec yields $DT^2 = 76T^2 \gg 1.4T$. At $\nu = 34.3$ kMc/sec, however, we expected a bottleneck similar to that in Sec. IV A. At this frequency $\Delta H \approx 20$ Oe, $D \approx 30$, and $A' \approx 250$, so that $AT \gg DT^2$. The data shown in Fig. 18 have a bad scatter but we still attempt to fit to $T_b^{-1} = DT^2 + C'T^9$ with the result $T_b^{-1} = 53T^2 + 3.5 \times 10^{-4} T^9$ sec^{-1}. However, a considerably better fit is found for the expression $T_b^{-1} = 176T + 6.1 \times 10^{-4} T^9$ sec^{-1}, indicating that the direct process is probably not bottlenecked, in contrast to the double nitrate case. The most likely explanation is that the ethyl sulfates are considerably less clear and so contain more defects, trapped liquid, etc., resulting in a value of T_{ph} given not by (51) but rather by the mean phonon lifetime for internal inelastic scattering, which would be $T_{ph} \lesssim 10^{-8}$ sec in this case.

V. SUMMARY AND CONCLUSIONS

A. Spin-Lattice Relaxation Time

In Table II are collected the theoretical estimates for the various relaxation rates for the five cases considered in Sec. IV, along with their measured values obtained by assuming $T_b^{-1} = T_1^{-1}$, except where a phonon bottleneck was detected, in which case the direct process is considered unmeasurable, although a lower limit can be set. For completeness sake, similar results of other workers are also included in the table for two additional cases of rare earth ions: Ce in the double nitrate[11,13,52,53] and Dy in the ethyl sulfate. (See Cooke et al.)[11]

It is seen that the temperature dependence of the direct, the Orbach, and the Raman processes are each amply demonstrated. Furthermore, the observed rates are mostly in remarkably good quantitative agreement with relatively simple theoretical estimates based on Orbach's phenomenological approach, thus amply establishing its validity and utility for rare earth ions. In this connection we note that the sums in Sec. IV of the type $\sum |\langle a | v_n{}^m | c \rangle|^2$ are all of the same order of magnitude,

[52] J. A. Cowen and D. E. Kaplan, Phys. Rev. 124, 1098 (1961).
[53] R. P. Hudson and B. W. Magnum (to be published) have also made relaxation time measurements on CeMN and NdMN by the audio-frequency susceptibility method.

TABLE III. Summary of results on the direct phonon bottleneck process DT^2 observed for rare earth ions in the double nitrate LaMN at $T \leq 1.5°K$.

	Ion					
	Pr	Pr	Nd	Sm	Ce[a]	Ce[a]
$c'=$ion concentration (%)	0.1/6	1/6	1	100	2	0.2
H (kOe)	6.88	6.88	9.1	17.3	3.75	3.75
$\Delta H=$linewidth (Oe)	15	15	6.5	100	8	4
ν (kMc/sec)	9.15	9.15	34.3	9.34	9.62	9.62
$\Delta\nu'=$linewidth (Mc/sec)	20	20	25	55	20	10
D, measured (sec^{-1} deg^{-1})	500	84	35	1.3	15	46
T_{ph}, from Eq. (74) (μsec)	0.63	0.37	0.18	0.11	0.17	0.28
$\tilde{l}=vT_{\mathrm{ph}}$ (cm)	0.16	0.093	0.046	0.027	0.042	0.07
$l=$crystal thickness (cm)	0.21	0.14	0.16	0.09	0.10	0.085
$\tilde{l}/l$	0.76	0.66	0.29	0.30	0.42	0.82

[a] Data from reference 13, Eqs. (6a), (6b).

the average being $\sim 7 \times 10^3$ cm^{-2}. Rough estimates for other rare earth ions not considered here can be quickly obtained by using this value in the general formulas in Sec. II. The field dependence $T_{1d}^{-1} \propto H^4$ for Kramers doublets has unfortunately not been explicitly demonstrated in our experiments because of the phonon bottleneck; however, the interpretation of the data in Sec. IV A and Sec. IV E is entirely consistent with this field dependence. The Orbach and Raman processes are demonstrated to be essentially field independent for the fields used here.

One gets the over-all impression from this table that for the rare earth ions at helium temperatures theory and experiment are in moderately satisfactory agreement, which is something that cannot yet be said for the iron group. Some reasons are: the rare earth theory is much simpler, J being a good quantum number; the experiments in Table II have been (purposely) done on simple level schemes, usually with only a single resonance line, thus avoiding the complication of multiple relaxation rates, cross relaxation, etc.; the phonon bottleneck has been detected and taken into account; the crystals have been mostly magnetically dilute and in fields large compared to the linewidths.

B. Phonon Bottleneck

Data for double-nitrate crystals are summarized in Table III for the four cases in Sec. IV where a direct phonon bottleneck was observed; in addition, we include two similar cases for Ce in LaMN from the following paper of Ruby, et al.[13] In each case a relaxation rate $T_b^{-1}=DT^2$ was observed at the lowest temperatures rather than the direct process $T_{1d}^{-1}=AT$. We rewrite Eq. (38a) as

$$T_{\mathrm{ph}}=2.6 \times 10^{-7}\Delta\nu'/c'D \text{ sec}^{-1}, \tag{74}$$

where $\Delta\nu'=$observed paramagnetic resonance linewidth in Mc/sec, $c'=$paramagnetic ion concentration in percent, $D=$measured value in sec^{-1} deg^{-2}. From this we calculate the mean hot phonon lifetime T_{ph}, obtaining the values shown, which range from 10^{-7} to 6×10^{-7} sec. We define a phonon path length $\tilde{l}=vT_{\mathrm{ph}}$ and compare it to the actual thickness l of the (flat) double-nitrate

crystals. The ratio $\tilde{l}/l$ ranges from 0.3 to 0.8, with an average value $(\tilde{l}/l)_{\mathrm{av}} \approx 0.54$. We note that this same value is obtained for crystals either immersed in liquid helium (Pr, Nd, and Sm), or glued inside an evacuated cold cavity (Ce).[13] Thus, T_{ph} may be interpreted as the time for sound waves to traverse the half-thickness of the crystals, in agreement with our earlier assumptions; the mechanism by which the phonons are cooled at first incidence is not known. There is a considerable scatter in $\tilde{l}/l$, however, and the crystal size has not been varied by more than a factor two; furthermore, diffusion effects have been neglected. Thus, an alternate interpretation is that T_{ph} represents the mean free time for internal inelastic scattering into high-frequency phonons. Since this should be frequency dependent, the experiments at 35 kMc/sec seem to contradict this for the double nitrate.

In all cases we have observed the bottleneck when $DT^2 \ll AT$, and failed to observe it when $DT^2 \gg AT$, in agreement with the predictions of Eqs. (39a,b). In summary, we feel that Table III along with the temperature dependence $T_b^{-1}=DT^2$ clearly establishes for the first time the existence of the phonon bottleneck.

As might be expected the most severe bottleneck is found for the non-Kramers doublet Pr. For 1% Pr in LaMN the observed bottleneck rate at 1.4°K is $\sigma \approx 10^3$ times smaller than the direct relaxation rate. From Eq. (40a) we estimate that our saturating pulse of 1 W peak power, corresponding to $s \approx 2$, produces a hot phonon temperature $T_p \approx 60°K$. After the pulse, this cools in a very short time $T_b' \approx 10^{-9}$ sec [cf. Eq. (38b)] to a value only a few tenths of a degree above the bath temperature. A pulse of 10^3 W would produce a hot phonon temperature $T_p \approx 10^3$ °K, which is not far below the theoretical maximum $T_p \approx \sigma T$ for complete saturation. Still higher phonon temperatures could be achieved by inverting the spin populations so as to get phonon maser action, as discussed by Townes[54] and demonstrated by Tucker.[55] Kittel[56] has noted the close relation

[54] C. H. Townes, *Quantum Electronics* (Columbia University Press, New York, 1960), pp. 405–409.
[55] E. B. Tucker, Phys. Rev. Letters **6**, 547 (1961).
[56] C. Kittel, Phys. Rev. Letters **6**, 449 (1961).

between a severe phonon bottleneck and the condition for the build-up of stimulated phonon emission, i.e., maser oscillations. In our notation this condition is, from Eq. (40c),

$$-n/n_0 \geq \sigma^{-1} \qquad (75)$$

so that only a fraction $\sigma^{-1} \approx 10^{-3}$ of the spins need inverting; such experiments are in progress here.

Paramagnetic Resonance below 1°K: Spin-Lattice Relaxation of Ce³⁺ and Nd³⁺ in Lanthanum Magnesium Nitrate*

R. H. RUBY, H. BENOIT,† AND C. D. JEFFRIES‡
Physics Department, University of California, Berkeley, California
(Received February 19, 1962)

An apparatus is described for performing paramagnetic resonance experiments at $\nu \approx 9.6$ kMc/sec at temperatures down to $T \approx 0.2°K$, obtained by adiabatic demagnetization. It is used to extend the spin-lattice relaxation rate T_1^{-1} measurements of the previous paper on Nd in the double nitrate $La_2Mg_3(NO_3)_{12} \cdot 24H_2O$ down to 0.3°K, where the direct process is very well displayed. For $z \perp H$ the result is $T_1^{-1} = 0.3 \coth(h\nu/2kT)$ sec⁻¹, to be compared to the theoretical estimate $T_1^{-1} = 0.6 \coth(h\nu/2kT)$ sec⁻¹. At the lowest temperatures the relaxation rate tends toward the temperature-independent value of spontaneous phonon emission.

For Ce in the double nitrate, the observed spin-bath relaxation rate T_b^{-1} at temperatures below 1°K is not the direct spin-lattice relaxation rate, but rather a phonon-limited bottleneck rate $T_b^{-1} \propto \coth^2(h\nu/2kT)$ which is concentration dependent. The results are consistent with the bottleneck rate $T_b^{-1} \propto T^2$ observed in the previous paper for other ions at higher temperatures. We find a lower limit for the true direct process $T_1^{-1} > 20 \coth(h\nu/2kT)$ sec⁻¹.

I. INTRODUCTION

ALTHOUGH microwave paramagnetic resonance experiments at temperatures T below 1°K have not yet been reported in detail, they are not without interest. Some phenomena which come to mind are: (1) The direct process for the spin-lattice relaxation rate T_1^{-1} in paramagnetic salts should become dominant over two-phonon processes and, if $h\nu \gg kT$, T_1^{-1} should become temperature independent, corresponding to spontaneous emission of phonons. (2) The phonon bottleneck may become appreciable.[1] (3) The Van Vleck linewidth of a resonance line should decrease as the spins become aligned at low temperatures,[2] and the line may become resolved into several sharp lines. (4) Spin ordering may set in due to dipolar interaction, or to exchange interactions even in magnetically dilute systems. (5) Starting temperatures $T \sim 0.2°K$ are useful in dynamic nuclear cooling experiments.[3]

To investigate these effects we have constructed a

paramagnetic resonance spectrometer operating at a frequency $\nu \approx 9.6$ kMc/sec and temperatures down to $T \approx 0.25°K$. In this paper we describe experiments concerning topics (1) and (2) above. They have been briefly reported earlier,[4] and are, to some extent, low-temperature extensions of the work described in the preceding paper[1] (referred to here as SJ), whose notation we use throughout.

II. APPARATUS

The essential details of the low-temperature paramagnetic resonance apparatus are given in Fig. 1. A long stainless steel evacuated can (shown cut-away) contains a cooling salt pill thermally linked to a microwave cavity. With the magnet in position A and the mechanical heat switch closed, the pill is cooled to $T_i \approx 1.5°K$ by the pumped He⁴ bath in a field $H_i \approx 9$ kOe. The switch is opened and the magnet lowered to position B, whereby the pill is cooled by adiabatic demagnetization to $T_f \approx 0.25°K$ for the salt used at present. Within a minute or so the cavity is also cooled to this temperature. The system then slowly warms up to 1.5°K over a period of 4 to 6 h, during which paramagnetic resonance experiments are performed on

* Supported in part by the Atomic Energy Commission and the Office of Naval Research.
† NATO Fellow.
‡ Associate Professor at the Miller Institute for Basic Research.
[1] P. L. Scott and C. D. Jeffries, preceding paper [Phys. Rev. 127, 32 (1962)].
[2] M. McMillan and W. Opechowski, Can. J. Phys. 38, 1168 (1960); 39, 1369 (1961).
[3] C. Kittel, Physica (Suppl.) 24, 588 (1958).

[4] R. H. Ruby, H. Benoit, P. L. Scott, and C. D. Jeffries, Bull. Am. Phys. Soc. II, 6, 512 (1961), paper J1.
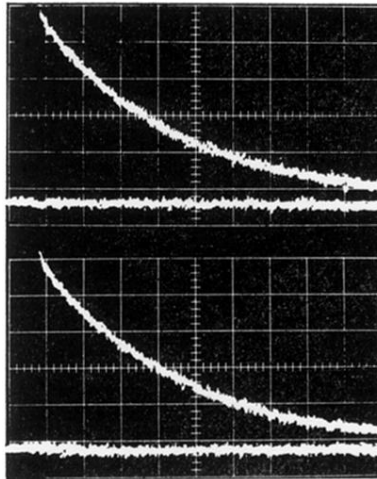
Fig. 3. Photographs of oscilloscope trace showing transient recovery of a spin resonance signal (0.5% Nd in La*ES* at 4.6°K) after saturation by a pulse. The ordinate is proportional to the i.f. detector voltage, the abscissa to time (10^{-3} sec per large division). The base line gives the final thermal equilibrium signal and is drawn by triggering the oscilloscope (but not the microwave switch) at a later time.